MEASURING THE REDUCTION POTENTIAL OF TAURINE:α-KETOGLUTARATE DIOXYGENASE AND BIOCHEMICAL ANALYSIS OF A THERMOPHILIC ORTHOLOG

Ву

Celeste Arlene Warrell

A THESIS

Submitted to
Michigan State University
in partial fulfillment of the requirements
for the degree of

Biochemistry and Molecular Biology - Master of Science

2013

ABSTRACT

MEASURING THE REDUCTION POTENTIAL OF TAURINE:α-KETOGLUTARATE DIOXYGENASE AND BIOCHEMICAL ANALYSIS OF A THERMOPHILIC ORTHOLOG

By

Celeste Arlene Warrell

This thesis seeks to determine the reduction potential, more specifically, the midpoint potential, of the archetypal non-heme iron/α-ketoglutarate dioxygenase, TauD, and to characterize a putative TauD ortholog from a moderately thermophilic bacterium. The accomplishment of these aims will expand our understanding of the mechanism of action of TauD and other members of this important enzyme superfamily. Two methods were employed to investigate the midpoint potential of TauD. Thin-layer cyclic voltammetry, an electrochemical method, was unsuccessful in directly generating a value for the midpoint of TauD. Instead, I used ultraviolet-visible spectroscopy to monitor titrations with the redox active dye methylene green to calculate the midpoint potential of Fe(III)/Fe(II)-TauD ($E_{\rm m}$ of -207 ± 27 mV vs. the Ag/AgCl electrode). Binding of the co-substrate α-ketoglutarate (0.5 mM) with and without the substrate taurine (0.5 mM) did not significantly shift this value (-204 ± 46 mV and -210 ± 32 mV, respectively). Preliminary activity assays suggested that the recombinant Mycobacterium thermoresistibile TauD-like protein is not a taurine:α-ketoglutarate dioxygenase. Ongoing studies by others are now examining an alternate function of this recombinant *M. thermoresistibile* protein as a sulfate-degrading enzyme.

ACKNOWLEDGEMENTS

First and foremost, I thank my mentor Dr. Bob Hausinger, for his amazing support, leadership, and guidance during my graduate career. I am blessed to have him as a mentor, not only a renowned scientist, who instills in his graduate students a rigorous and careful scientific training, but who is also genuinely concerned with his students. Bob's full-hearted support is a gift I can never repay, but one I will appreciate the rest of my life. I gratefully acknowledge my committee members Drs. Denis Proshlyakov, Eric Hegg, Charles Hoogstraten, and Shelagh Ferguson-Miller for their guidance and support. I thank Dr. Denis Proshlyakov in particular for his close collaboration in the work described in this thesis, for his guidance as an expert in this field, and for his aid in my scientific training. I am indebted to all the members of the Hausinger lab I have been privileged to meet, for their advice, helpful scientific discussions, support and constant encouragement, especially, Dr. Scott Mulrooney, Dr. Tina Müller, Dr. Lee Macomber, and Mark Farrugia, my lab family. I also wanted to thank in a particular way Stephanie DeDore, an undergraduate student who assisted me in my studies of the *M. thermoresistibile* protein. In addition, I acknowledge all those who have previously worked on TauD, laying the groundwork for this project. Finally, I thank my family and friends for their love and support; these are blessings I truly treasure.

TABLE OF CONTENTS

LIST OF TABLES	∕i
LIST OF FIGURESv	/ii
KEY TO ABBREVIATIONS	χi
INTRODUCTION	.1
CHAPTER 1. ELECTROCHEMISTRY OF TAUD: THIN-LAYER CYCLIC VOLTAMMETRY Materials and Methods Purification of TauD Activity Assays TLCV	7 .7 8 9
Results and Discussion	20
Materials and Methods	20 .21
Results and Discussion	23
TauD Determination of the Midpoint Potential of TauD in the Presence of	.24
CHAPTER 3. CLONING, EXPRESSION, AND PROPERTIES OF A TAUD ORTHOLOG FROM A THERMOPHILE	43 43
E. coli Purification Activity Assays Results Discussion.	.45 .46 .46

REFERENCES	F	50)
		"	_

LIST OF TABLES

Table 1. Measured midpoint potentials of Fe(III)-/Fe(II)-TauD alone, with	0.5 mM
α -KG, and with 0.5 mM α -KG and 0.5 mM taurine. All reported midpoint po	otentials are
in reference to the Ag/AgCl reference electrode.	39

LIST OF FIGURES

Figure 1. Simplified reaction mechanism of TauD. The Fe center is colored in blue and the oxygen atoms derived from molecular oxygen are colored in red for clarity. For interpretation of the references to color in this and all other figures, the reader is referred to the electronic version of this thesis. Adapted from Grzyska <i>et al.</i> [1]
Figure 2. TLCV of Fe(II)-TauD alone, ferricyanide alone, and a mixture of these species. For interpretation of the references to color in this and all other figures, the reader is referred to the electronic version of this thesis. The samples were poised at the lowest potential shown for 100 s and scanned at 1 mV/s while monitoring the current. The samples included buffer as a blank (black trace), 230 μM holoenzyme alone (red trace), 50 μM ferrocyanide (blue trace), or a mixture of these two species (49 μM ferrocyanide plus 226 μM holoenzyme) (green trace (8/8/12)
Figure 3. TLCV of methyl viologen and Fe(II)-TauD with methyl viologen. The samples were poised at the lowest potential for 100 s and scanned at 10 mV/s while monitoring the current. Panel A: buffer (black trace), 494 μ M methyl viologen (red trace), and 382 μ M mediator with 196 μ M holoenzyme (blue trace). Panel B shows the same samples of mediator and holoprotein re-injected into the electrochemical cell in a second run (8/13/12).
Figure 4. TLCV of methylene green and Fe(II)-TauD with methylene green. A buffer control was poised at low potential for 2 s and scanned at 10 mV/s while monitoring the current (black trace). The samples were poised at the lowest potential for 100 s and scanned at 10 mV/s. These included 225 μ M holoprotein (red trace), 499 μ M methylene green (blue trace), and 500 μ M mediator and ~200 μ M holoprotein (green trace) (8/29/12)
Figure 5. TLCV of Fe(II)-TauD with methylene green at various scan rates. Samples were poised at the lowest potential shown for 100 s (or 2 s for a buffer blank) and scanned. The samples included a buffer blank (black trace, 10 mV/s) or 500 μ M methylene green with ~200 μ M holoprotein scanned at 2 mV/s (red trace), 5 mV/s (blue trace), or 10 mV/s (green trace) (8/29/12).
Figure 6. TLCV of Fe(II)-TauD with methylene green at a very slow sweep rate and a high protein:mediator ratio. Samples were poised at low potential for 300 s and scanned at 0.2 mV/s while monitoring the current. The samples included 52 μ M methylene green (black trace), the same concentration of mediator and 418 μ M holoprotein (red trace), and the mixture repeated on the next day (blue trace) (9/24/13).
Figure 7. TLCV of methylene blue and Fe(III)-TauD with methylene blue. The samples were poised at low potential for 2 s and scanned at 2 mV/s while monitoring the current. The samples were 50 μ M methylene blue alone (black trace) and 50 μ M methylene blue plus 90 μ M Fe(III)-TauD (red trace) (12/3/12)

Figure 8. Absolute spectrum of reduced and air-oxidized methylene green. Methylene green (~4 μM) was ~90% reduced with an aliquot of sodium dithionite from a 250 mM stock solution (black trace). Ensuing traces represent spectra obtained after oxygen was injected into the anaerobic cuvette, and waiting various times for oxygen to react with methylene green. The solution was constantly stirred during acquisition of the spectra.)
Figure 9. Difference spectra of air-oxidized and reduced methylene green. The spectra obtained during sample oxidation in Figure 8 were subtracted from the spectrur of the reduced sample.	
Figure 10. Kinetics of the reaction of reduced methylene green with Fe(III)-TauD plus 0.5 mM α-KG. The protein sample (20 μM) in 25 mM Tris, pH 8, was amended with increasing concentrations of methylene green from a 0.5 mM stock solution with stirring and at room temperature. Absolute spectrum of blanked protein (black trace) and increasing amounts of ~90% reduced MG titrated into the protein (traces in color). Absorbances were not corrected for dilution. For this titration, the amount of oxidized methylene green was calculated from the difference in corrected absorbances at 664 nm and 850 nm (4/23/13).	1
Figure 11. Absolute spectrum of the titration of methylene green into Fe(III)-TauD The protein sample (20 μM) in 25 mM Tris, pH 8, was amended with increasing concentrations of methylene green from a 0.5 mM stock solution with stirring and at room temperature. Absolute spectrum of blanked protein (black trace) and increasing amounts of ~90% reduced MG titrated into the protein (traces in color). Absorbances were not corrected for dilution. For this titration, the amount of oxidized methylene gree was calculated from the difference in corrected absorbances at 664 nm and 850 nm (4/23/13).	n
Figure 12. Titration of reduced methylene green into Fe(III)-TauD. Profiles are	
shown for wavelengths corresponding to oxidized methylene green (A _{664 nm} - A _{850 nm}) and reduced mediator (A _{260 nm} – A _{291 nm}) when reduced methylene green was titrated into buffer (green triangles and blue X, respectively) or into a solution containing 20 μM Fe(III)-TauD (blue diamonds and red boxes, respectively). The absorbances were corrected for dilution	t
Figure 13. Titrations of ~90% reduced methylene green into solutions of Fe(III)-TauD while monitoring the concentrations of oxidized methylene green. Four replicates (blue traces with markers) are shown along with their fits (red traces). The estimated E_m values for the holoprotein (vs. Ag/AgCl electrode) in these experiments were: -227 ± 3 mV (Panel A, 20 μ M protein, 4/23/13), -215 ± 5 mV (Panel B, 10 μ M protein, 7/3/13), -187 ± 10 mV (Panel C, 20 μ M protein, 7/4/13) (Panel C), and -187 ± 7 mV Panel D, 15 μ M protein, 7/10/13)	

Figure 14. Titrations of ~90% reduced methylene green into solutions of Fe(III)- TauD plus α-KG while monitoring the concentrations of oxidized methylene
green. Three replicates are shown along with their fits. The estimated E_m values for the holoprotein (vs. Ag/AgCl electrode) in these experiments containing 0.5 mM α-KG were -218 ± 2 mV (Panel A, 20 μM protein, 7/8/13) and -255 ± 6 mV (Panel B, 15 μM protein, 7/11/13), and -165 ± 27 mV (Panel C, 10 μM protein, 7/12/13)
Figure 15. Titrations of ~90% reduced methylene green into solutions of Fe(III)-TauD, α-KG, and taurine while monitoring the concentrations of oxidized
methylene green. Two replicates are shown along with their fits. The estimated E_m values for the holoprotein (vs. Ag/AgCl electrode) in these experiments containing 0.5 mM α-KG and 0.5 mM taurine were: -179 ± 9 mV (Panel A,10 μM protein, 7/5/13) and -218 ± 4 mV (Panel B, 15 μM protein, 7/12/13)
Figure 16. Alternative scheme of the decomposition of Fe(IV)-oxo intermediate and formation of products. Instead of radical rebound from an Fe(III)-OH species taking place to form the products (top arrows), Raman spectroscopic analyses provided evidence consistent with formation of an Fe(III)-O ⁻ intermediate and putative Fe(II)-alkoxo species (bottom arrows) that generate the products. Adapted from Grzyska <i>et al.</i> [1]
Figure 17. Initial expression of <i>Mth</i> TauD-like protein in the supernatants of lysed <i>E. coli</i> BL21(DE3) cells over various induction conditions. From left to right on the 12% SDS-PAGE gel. Lane 1: Prestained molecular mass standards (BioRad). Subsequent lanes are divided into 3 sets of conditions, with a skipped lane in between the first and second and before the third set. Lanes 2-4 contain cell extracts of cells grown at 16 °C after induction, Lanes 6-8 grown at room temperature after induction,
and Lanes 10-12 grown at 35 °C after induction. Lanes, 2, 6, and 10 contain extracts from cells induced with 0.25 mM IPTG (final concentration), Lanes 3, 7, and 11 contain those induced with 0.5 mM IPTG, and Lanes 4, 8, and 12 contain those induced with 1 mM IPTG. Note: Molecular mass standards were not boiled prior to gel electrophoresis, while the samples were boiled
Figure 18. 12% SDS-PAGE gel of fractions eluting from a DEAE-Sepharose column. The first lane shows prestained molecular mass standards (BioRad) and subsequent lanes show fractions from the column. Lanes 6-10 contain enriched <i>Mth</i> protein. Note: Molecular mass standards (in kDa) were not boiled prior to gel electrophoresis, while the samples were boiled.
Figure 19. Sequence alignment of <i>E.coli</i> TauD with three <i>Mycobacterium</i> putative dioxygenases. <i>M. thermoresistibile</i> ATCC 19527 (sequence 2), and <i>M. tuberculosis</i> Rv0097 (sequence 3) and Rv3406 (sequence 4) are aligned to <i>E. coli</i> TauD (sequence 1). Conserved ligands of Fe are underlined and bolded. Residues in <i>E. coli</i> TauD crucia for binding taurine are marked with an asterisk

Figure 20. Taurine bound in the crystal structure of TauD with α-KG. Bound tauri	ine
(center) with hydrogen bonds (black dashes) to relevant residues. Residues of interes	st
are shown as sticks. Fe in the active site is represented as a brown sphere. Oxygen	
atoms are shown in red, nitrogen atoms in blue, and carbon atoms in green. Generate	ed
from Pymol using PDB ID 1GY9.	.5

KEY TO ABBREVIATIONS AND SYMBOLS

Taurine:α-ketoglutarate dioxygenase	TauD
α-ketoglutarate	α-KG
Tris(hydroxymethyl)aminomethane	Tris
Ethylenediaminetetraacetic acid	EDTA
Phenylmethylsulfonylfluoride	PMSF
Diethylaminoethyl-Sepharose	DEAE-Sepharose
Isopropyl β-D-1-thiogalactopyranoside	IPTG
Thin-layer cyclic voltammetry	TLCV
Cyclic voltammogram	CV
Ultraviolet-visible spectroscopy	UV-Vis Spectroscopy
Midpoint potential	<i>E</i> m
Dithiothreitol	DTT
Normal hydrogen electrode	NHE
2,4-Dichlorophenoxyacetic acid/α-KG dioxygenase	TfdA

INTRODUCTION

Non-heme Fe(II)/α-ketoglutarate (α-KG)-dependent dioxygenases comprise a superfamily of enzymes with diverse biological roles [2-7]. For example, specific representatives function in the repair of alkylated DNA, synthesis or catabolism of a wide range of molecules, and regulation of the hypoxic response. Correspondingly, mutations in genes encoding various enzymes of this superfamily are associated with a variety of human diseases. Thus, deficiencies in prolyl 4-hydroxylase lead to defects in connective tissue in mammals [8], and amino acid substitutions in phytanoyl-coenzyme A 2-hydroxylase can cause Refsum disease, a neurological disorder [9]. Of great importance are the members involved in the synthesis of antibiotics, such as bacterial clavaminate synthase [10]. Similarly, plant Fe(II)/ α -KG-dependent dioxygenases serve many roles including synthesis of the flavonoid hormones, which have been studied for their possible anti-cancer drug ability [11]. Knowledge of the mechanism of action of these enzymes is of great biological significance, as a more detailed mechanistic understanding may lead to the treatment of these human diseases or the design of novel catalytic functions.

The great versatility in the range of substrates utilized by these enzymes is mirrored in the diverse types of chemical reactions they catalyze. For example, in addition to the commonly observed hydroxylation chemistry there are representatives which catalyze halogenation, epoxidation, racemization, ring formation, and ring expansion reactions, all carried out by the same type of mononuclear Fe(II) center [2].

The Fe(II)/ α -KG dioxygenases all coordinate their mononuclear Fe(II) centers by using two conserved histidines and a conserved aspartate or glutamate in what is

known as a "2-His-1-carboxylate" facial triad [12]. In the absence of substrate and cosubstrate, three solvent water molecules occupy the remaining sites in an octahedral coordination sphere. The co-substrate α-KG serves as an electron donor to the catalytic cycle in the enzyme-catalyzed oxidation reactions (i.e., the co-substrate undergoes oxidative decarboxylation), and it primes the enzyme active site for reaction with molecular oxygen. Subsequent steps of catalysis are best studied in the *Escherichia coli* enzyme known as TauD or taurine:α-KG dioxygenase [13]. The cell uses TauD to metabolize taurine as an alternative sulfur source under sulfur-deficient conditions [14]. This enzyme can be stably isolated in large quantities and has been subjected to extensive spectroscopic studies consistent with the catalytic cycle shown in Figure 1.

Catalysis begins when the co-substrate α-KG binds to Fe(II) in the resting enzyme (A), displacing two coordinating solvent molecules (B). Taurine binds to the enzyme next (C), displacing the last water molecule, but does not coordinate the metal ion. The active site is now primed to bind and activate molecular oxygen. Dioxygen binds, forming a proposed Fe(III)-superoxide intermediate (D), followed by formation of a putative bicyclic Fe(IV)-peroxo species (E). Decarboxylation of the coordinating α-KG forms a catalytically potent oxidant, the Fe(IV)-oxo species (F), an intermediate observed through Mössbauer [15], X-ray absorption [16], and resonance Raman spectroscopy [17]. This Fe(IV)-oxo species is proposed to abstract a hydrogen atom from the C1 carbon of taurine, creating a substrate centered radical and an Fe(III)-OH species (G). According to the classical mechanism, the product is formed upon hydroxyl radical rebound to form hydroxylated taurine, which immediately decomposes into aminoacetaldehyde and sulfite; however, time-dependent continuous-flow cryogenic

(-36 °C) Raman analyses suggest two additional intermediates exist at this stage that were tentatively identified as an Fe(III)-oxo and an Fe(II)-alkoxo species (not depicted in Figure 1) [1]. Succinate, the second byproduct of α -KG, is released at the end of the catalytic cycle, and the Fe(II)-resting state of the enzyme is regenerated.

The work described in thesis seeks to expand our understanding of TauD catalysis. Chapters 1 and 2 use two independent approaches, thin-layer cyclic voltammetry (TLCV) and ultraviolet-visible (UV-Vis) spectroscopy, to examine the reduction potential of the enzyme metallocenter. My hypothesis is that the electrochemical properties of the iron center, specifically the reduction potential of the metallocenter, affect the reactivity and kinetics of the individual steps in catalysis [18].

The reduction potential of the enzyme is defined by Equation 1, where E^o is the standard reduction potential under non-physiological conditions. As an alternative to this parameter, I examined the midpoint potential, the reduction potential at which the concentration of oxidized species equals the concentration of the reduced species, a measure of the equilibrium properties of the reaction.

$$E = E^{0} - (RT/nF) \ln ([M_{red}]/[M_{ox}])$$
 (Eq. 1)

The midpoint potential has not been reported for any Fe(II)/ α -KG dioxygenase, so knowledge gained using TauD will be important for its application to other members of the non-heme iron oxygenase family. Measurement of the midpoint potential will give insights into how the protein environment affects the redox properties of the metal compared to protein-free iron [18, 19]. In addition, the effects of the electron-donating co-substrate α -KG and the substrate taurine on the midpoint potential will be examined. I expect the electron-donating α -KG ligand to decrease the midpoint potential (to a more

negative value) while substrate binding may also have an effect as the metal changes from six-coordinate to five-coordinate geometry.

Chapter 3 describes my preliminary efforts to purify and characterize a TauD paralog from a thermophilic microorganism. My hypothesis is that by using an enzyme designed to operate at elevated temperatures one can carry out transient kinetic analysis without resorting to cryogenic conditions and perhaps better examine the intermediate species during catalysis.

Figure 1. Simplified reaction mechanism of TauD. The Fe center is colored in blue and the oxygen atoms derived from molecular oxygen are colored in red for clarity. For interpretation of the references to color in this and all other figures, the reader is referred to the electronic version of this thesis. Adapted from Grzyska *et al.* [1].

CHAPTER 1. ELECTROCHEMISTRY OF TAUD: THIN-LAYER CYCLIC VOLTAMMETRY

Taurine: α -ketoglutarate (α -KG) dioxygenase, or TauD, the best characterized member of the non-heme Fe(II)/ α -KG-dependent dioxygenase superfamily, was examined by electrochemical methods in an effort to determine its midpoint potential.

Direct protein electrochemistry has been used to measure electron transfer reactions and redox potentials of many proteins [20-22]. These methods include adhering the protein of interest directly to an electrode in an electrochemical cell, scanning over a range of potentials, and relating the measured current to the protein's redox potential; e.g., this approach was recently utilized to investigate hydrogenases [23]. However, direct electrochemistry of the TauD metallocenter is unlikely to be effective due to the inaccessibility of the buried iron site which is sandwiched in an 8stranded dual β-sheet in what is termed a double-stranded β-helix or a jellyroll fold [24]. Nevertheless. I describe the results of using direct electrochemical methods with this enzyme. As an alternative electrochemical approach to examine the metallocenter redox properties I use indirect electrochemistry, a technique that employs a mediator, or small redox active compound, to shuttle electrons between a protein metallocenter and the electrode [21, 25]. Ideally, a mediator of the appropriate redox potential will interact with the TauD metallocenter and conduct electrons between the metallocenter and the electrode. An appropriate mediator will have a redox potential similar to that of TauD to obtain the most accurate estimate of the protein potential.

In this research, I collaborated with Dr. Zipin Zhang and Christopher John in Dr. Denis Proshlyakov's lab to explore using thin-layer cyclic voltammetry (TLCV) to determine the midpoint potential of the Fe(III)/Fe(II)-TauD couple. As the name implies,

TLCV utilizes a thin layer of solution spread over the electrode's surface, so the diffusion distance between the surface and the redox active metallocenter is minimized [25, 26]. Consequently, the electron transfer rate is not limited by the diffusion of the electron donor or acceptor to the iron site.

Materials and Methods

Purification of TauD

TauD was expressed from the plasmid pME4141 in Escherichia coli BL21(DE3) cells (Agilent) that were grown in six 1-L cultures of Terrific Broth medium (Fisher-Scientific) containing 50 µg/mL kanamycin at 37 °C. The cells were shaken at 200-220 rpm until reaching an optical density (OD₆₀₀) of ~0.5-0.7, induced with 1 mM isopropyl β-D-1-thiogalactopyranoside (IPTG), and grown at 30 °C overnight (~14-18 h). Harvested pellets were usually divided into two or three different tubes and frozen at -80 °C until needed for enzyme isolation. For protein purification, thawed pellets were resuspended in 20 mM Tris/1 mM phenylmethylsulfonylfluoride (PMSF)/1 mM ethylenediaminetetraacetic acid (EDTA), pH 8, and sonicated for 5 cycles (Branson Sonifier 450) using output control 2-3, at a duty cycle of 50%, for 2 min each time. Sonicated pellets were ultracentrifuged at approximately 33,000 x g for 1 h. The supernatants of this spin, termed "cell extracts", were loaded onto a cation exchange diethylaminoethyl (DEAE)-Sepharose column (there were two DEAE-Sepharose columns I used, either a 2.5 cm diameter by 16.5 cm in length or a 2.5 cm X 12 cm column) in 25 mM Tris/1 mM EDTA, pH 8, and eluted in a high salt gradient (1 M NaCl in 25 mM Tris, pH 8). Pooled TauD was bound to a phenyl-Sepharose column (2.5 X 12 cm) in buffer containing 0.5 M

(NH₄)₂SO₄, and the column was developed with a decreasing (NH₄)₂SO₄ gradient followed by a wash with water. Some TauD eluted in the low salt region of the gradient in 25 mM Tris, pH 8, but the majority of the bound TauD eluted in water. The latter sample was collected as 4-mL fractions in test tubes containing 4 mL 50 mM Tris, pH 8, and dialyzed overnight in 25 mM Tris, pH 8 to maintain stability. The pooled fractions were judged to be 90-98% TauD on the basis of sodium dodecyl sulfate (SDS)-polyacrylamide gel electrophoresis (PAGE) using 5% stacking and 12% running gels [27]. Gel filtration chromatography using a Superdex-200 column (1.5 X 64 cm) equilibrated in 150 mM NaCl in 25 mM Tris buffer, pH 8, was used as a final purification step. Pooled protein from each column was concentrated with 15-mL centrifugal filters (Millipore) using a molecular weight cutoff (MWCO) of 10 kDa.

Activity Assays

The purified TauD was assayed for activity in a protocol loosely based on what has been previously described [14], with the following exceptions. The activity assays were carried out at 37 $^{\circ}$ C in a master mix containing 1 mM taurine, 0.5 mM α -KG, and 25 mM Tris, pH 8. The amount of protein added to the master mix ranged from 2-10 µg/mL (to ensure that the measured absorbance at 415 nm would fall within the linear range of the sulfite calibration curve). Aliquots from stock solution of 5 mM Fe(NH₄)(SO₄)₂/ 10 mM ascorbate (in water) were added to the master mix to initiate the reaction to give a final concentration of 1 mM Fe(II)/ 2 mM ascorbate. The reaction was quenched at 0.5, 1, 2, 3, 4, and 5 min by the addition of 0.1 mL of 0.5 M EDTA. The absorbances at 415 nm of the reacted solutions were measured \sim 0.5-2 min after the

addition of 0.1 mL of 1 mg/mL 5,5'-dithiobis(2-nitrobenzoic acid) (Ellman's reagent). The specific activity was calculated from the amount of sulfite produced, with purified TauD ranging across different experimental preparations from 7-11 U/mg (fresh, unfrozen enzyme) and \sim 2-4 U/mg (frozen enzyme, then thawed for activity assays), where 1 U is defined as 1 µmol sulfite produced in 1 min at 37 $^{\circ}$ C.

TLCV

Purified apoprotein was degassed by using eighteen cycles of 10 s vacuum followed by 10 s Ar purge per cycle. Degassed Fe(NH₄)₂(SO₄)₂ (Fisher Scientific) was added to apoprotein to obtain approximately 90% loaded Fe(II)-TauD. In the experiments with various mediators, a dilute solution of mediator and a mixture of holoenzyme plus mediator were each prepared in 0.2 M KCl in 25 mM Tris, pH 8. The identities and concentrations of the mediators used in each experiment are related in the Results and Discussion portion of this section and in the corresponding figure legends.

The thin-layer spectroelectrochemical cell and its set-up has been previously described [26]. The three-electrode set-up consisted of boron-doped diamond electrode as the working electrode, a platinum wire as the counter electrode, and Ag/AgCl as the reference electrode. The cell was equipped with a spacer to give it a 75 µm thickness. Prior to loading of samples, the interior of the cell was thoroughly rinsed with buffer (0.2 M KCl in 25 mM Tris, pH 8). Degassed buffer was loaded from a gas-tight syringe via the buffer loading port. As a blank, the potential of the buffer alone was measured under the same conditions and parameters for which the sample was examined. Samples were loaded with a gas-tight syringe by injection of 100 µL of solution into the

cell via the sample loading channel. The cell was connected to a potentiostat (Model 760B, CH Instruments, Inc., Austin, TX) to control the applied potential.

Depending on the initial oxidation state of the protein and the mediator, the electrochemical cell was correspondingly set at initially oxidizing or reducing conditions. If both protein and mediator were prepared in their oxidized states, the potential of the cell was initially set at a high value and then decreased to lower values before returning to the initial potential (reducing conditions followed by oxidizing conditions). If the protein and mediator solutions were prepared in their reduced states, the potential of the cell was initially set at a low value and then increased before returning to the initial value (oxidizing conditions followed by reducing conditions). The period of the run in which the electrochemical cell's potential increases is referred to as the oxidation sweep, while the period in which the cell's potential decreases is referred to as the reduction sweep. The scan rate over different experiments varied from 0.2 mV/s to 10 mV/s.

For direct electrochemistry, I used the voltammogram readout from TLCV to estimate the midpoint potential as the midpoint of the maxima from the oxidative and reductive sweeps. To analyze the data for indirect electrochemistry involving mediators, I used the approach described by Parker and Seefeldt [25], in which the midpoint potentials of the mediator and the metallocenter could theoretically be separately distinguished.

Results and Discussion

Direct electrochemistry of TauD by TLCV was examined; however, no current was detected (Figure 2, red trace). These results are consistent with the metallocenter

being buried in the protein and inaccessible to the electrode, resulting in a very slow rate of electron transfer. Given these results, I switched to an indirect electrochemical approach to probe the TauD midpoint potential using mediators.

Four mediators were employed in TLCV studies: ferro-/ferricyanide, methyl viologen, methylene green, and methylene blue. As described in greater detail below, and in contrast to expectations based on the report by Parker and Seefeldt [25], none of the TLCV experiments resulted in distinct sets of oxidation/reduction features corresponding to the mediator potential(s) and a separate potential for TauD.

Consequently, the midpoint potential of Fe(III)/Fe(II)-TauD could not be determined by the simplistic approach of analyzing the cyclic voltammograms according to the average of the oxidation and reduction potential values.

Electrochemical studies with ferrocyanide are summarized in Figure 2. Examination of the mediator alone under the stated conditions yielded a CV (blue scan) with the expected appearance; i.e., a maximal positive current at +0.27 V, and maximal negative current at +0.15 V, corresponding to $E_{\rm m}$ of +0.21 V (at pH 8). This result is slightly shifted when compared to the literature $E_{\rm m}$ of +0.286 V (vs. Ag/AgCl, glassy carbon working electrode, 0.25-1 mM ferricyanide dissolved in 1 M KCl in water, 1-20 mV/s) [26]. When a mixture of ferrocyanide plus Fe(II)-TauD was scanned (green scan), an increase in the total current was detected in the oxidative sweep. As the potential decreased, the reduction peak position shifted to a more negative value, and the amplitude of the measured current decreased. A signal unique to protein was not detected. This result was counter to the hypothesis that the mediator's midpoint potential would be unaffected while allowing visualization of the midpoint potential for

the protein. It may be that the ferricyanide directly interacts with amino acid residues in TauD, rather than the iron in the protein's active site. Alternatively, these results hinted that the electrochemical behavior of a metalloprotein and mediator as claimed by Parker and Seefeldt [25] was oversimplified. CV studies of the reverse reaction, starting with Fe(III)-TauD and ferricyanide, also failed to produce a peak unique to protein reduction or oxidation. Rather, the CV of a mixture of ferricyanide and Fe(III)-TauD appeared the same as the CV of ferricyanide alone (data not shown). This result suggests that ferricyanide does not interact with the oxidized metallocenter of TauD.

Electrochemical studies using methyl viologen are shown in the two panels of Figure 3. Analysis with mediator alone (red traces) yielded CV traces that allowed estimations of two $E_{\rm m}$ values of ~-0.7 V and ~-1.1 V (vs. Ag/AgCl, pH 8 because methyl viologen is able to undergo either a one- or two-electron transfer [28]). A preliminary trial using a mixture of enzyme and methyl viologen provided a CV that included a separate peak during the oxidation sweep (top spectrum, blue trace), but this feature was not reproducible. Rather, the CV for the sample of holoprotein plus mediator was almost identical to the CV of methyl viologen alone (lower panel, blue and red traces, respectively), but with the protein leading to decreased intensities. This result may be attributed to the midpoint potentials of methyl viologen being too distant (too negative) from the midpoint potential of TauD to interact with the metallocenter of the protein. Consequently, TLCV studies with methyl viologen as a mediator were discontinued.

TLCV studies with methylene green (Figure 4) provided two midpoint potentials for the mediator ($E_{m1} \sim -0.24$ V and $E_{m2} \sim -0.13$ V, blue trace), in agreement with the literature ($E_{m1} = -0.20$ V and $E_{m2} = -0.05$ V vs. Ag/AgCl) [29, 30]. Initial trials for a

mixture of 500 μM methylene green and ~200 μM Fe(II)-TauD appeared promising, with more current detected in the protein/mediator mixture than in the scan with methylene green alone (green trace). In follow-up experiments, the protein concentration was increased relative to methylene green concentration to augment any potential protein signal in the CV (Figure 5) and the scan rate was decreased to minimize peak separation of the mediator oxidative and reductive maxima and to reduce distortion of whatever protein signal might be observed (Figure 6). However, these attempts to optimize the conditions of the TLCV measurement did not provide a protein signal that was distinct from the oxidation/reduction peaks of methylene green. At best, there was an increase in the current in the presence of protein, indicating that more charge was transferred to the electrode in the protein/mediator mixture.

Methylene blue TLCV studies (Figure 7, black trace) yielded a midpoint potential of \sim -0.33 V vs. the Ag/AgCl electrode (E^0 = -0.23 V vs. the normal hydrogen electrode (NHE), which corresponds to -0.435 V vs. the Ag/AgCl electrode [31-33]). When the mediator was mixed with protein and scanned (red trace), an interaction with the TauD metallocenter was evidenced by the increase in the detected current of the CV of the methylene blue/Fe(III)-TauD mixture relative to the CV of methylene blue alone. This increase in current indicated that more charge, thus more electrons, was conducted to the electrode in the presence of enzyme; however, no signal unique to TauD was detected.

Despite varying the identity of the mediators, scan rates, protein/mediator concentrations, and the relative protein/mediator ratio, no unique set of peaks could be assigned to the oxidation and reduction of TauD. A lower scan rate (0.2 mV/s)

decreased the separation between reduction and oxidation peaks in the voltammogram, but also decreased the amplitude of the measured current. An increase in the current of the CVs for the mixture of protein and mediator compared to mediator alone was consistently observed with methylene green and methylene blue, suggesting that these mediators transfer electrons to and from the protein-coordinated iron; however, no oxidation/reduction pair of peaks unique to the enzyme could be detected.

In conclusion, my attempts to estimate directly the midpoint potential of TauD by analysis of separate protein-dependent features in TLCV were unsuccessful. My results call into question the analysis method that assumes the mediator and metallocenter distinct midpoint potentials are readily resolved [25] and demonstrate that this method does not apply to TauD. I have provided protein samples and assisted Christopher John in additional TLCV studies that do not make this assumption, but that ongoing effort using more sophisticated analytical approaches is not described here. As an alternative approach to assess the enzyme's midpoint potential, I examined a UV-visible spectroscopy technique that is detailed in the next chapter.

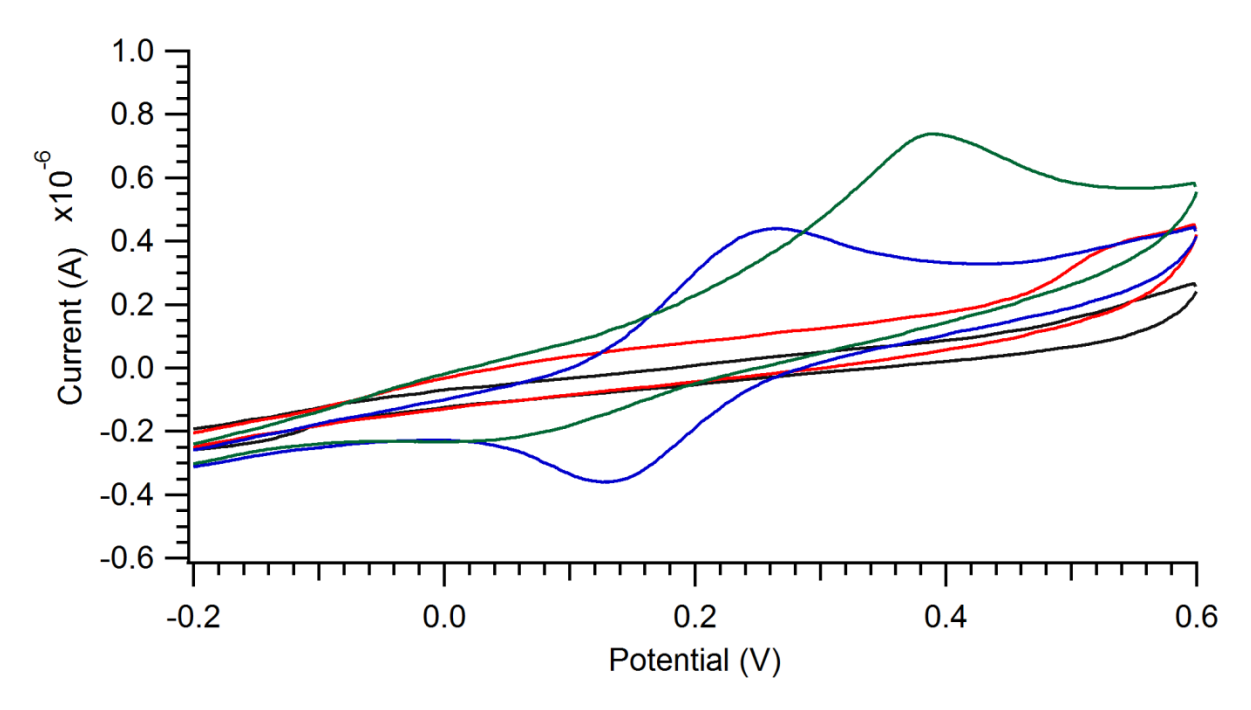
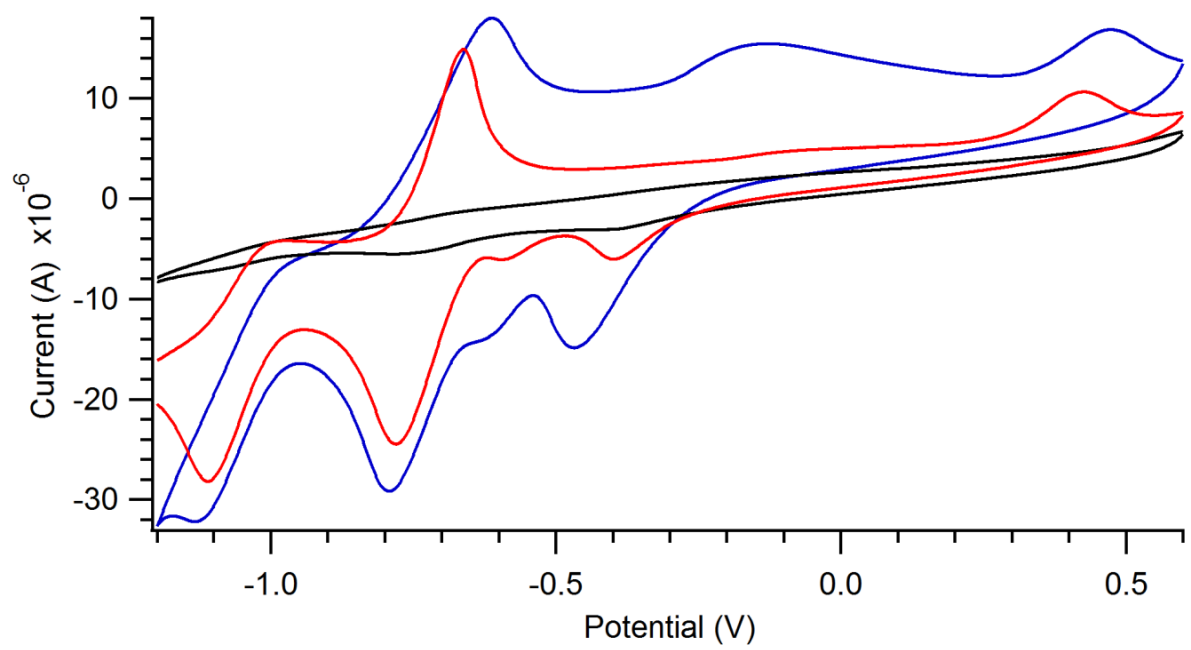


Figure 2. TLCV of Fe(II)-TauD alone, ferrocyanide alone, and a mixture of these species. For interpretation of the references to color in this and all other figures, the reader is referred to the electronic version of this thesis. The samples were poised at the lowest potential shown for 100 s and scanned at 1 mV/s while monitoring the current. The samples included buffer as a blank (black trace), 230 μ M holoenzyme alone (red trace), 50 μ M ferrocyanide (blue trace), or a mixture of these two species (49 μ M ferrocyanide plus 226 μ M holoenzyme) (green trace (8/8/12).

Panel A



Panel B

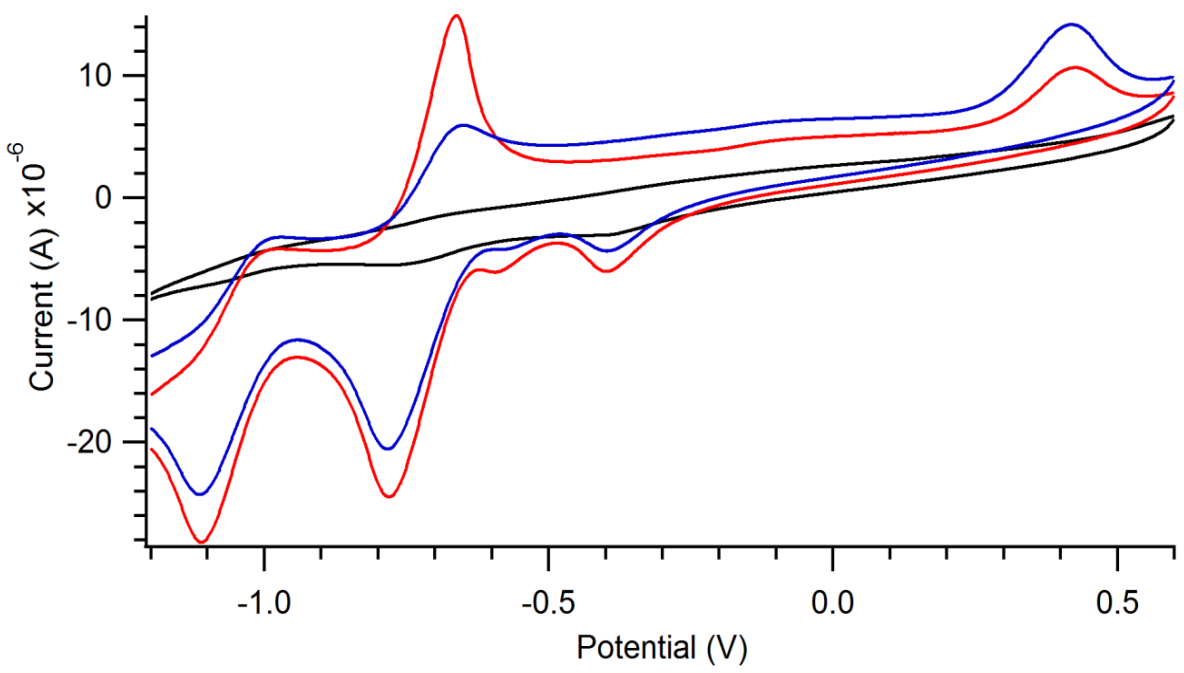


Figure 3. TLCV of methyl viologen and Fe(II)-TauD with methyl viologen. The samples were poised at the lowest potential for 100 s and scanned at 10 mV/s while monitoring the current. Panel A: buffer (black trace), 494 μ M methyl viologen (red trace), and 382 μ M mediator with 196 μ M holoenzyme (blue trace). Panel B shows the same samples of mediator and holoprotein re-injected into the electrochemical cell in a second run (8/13/12).

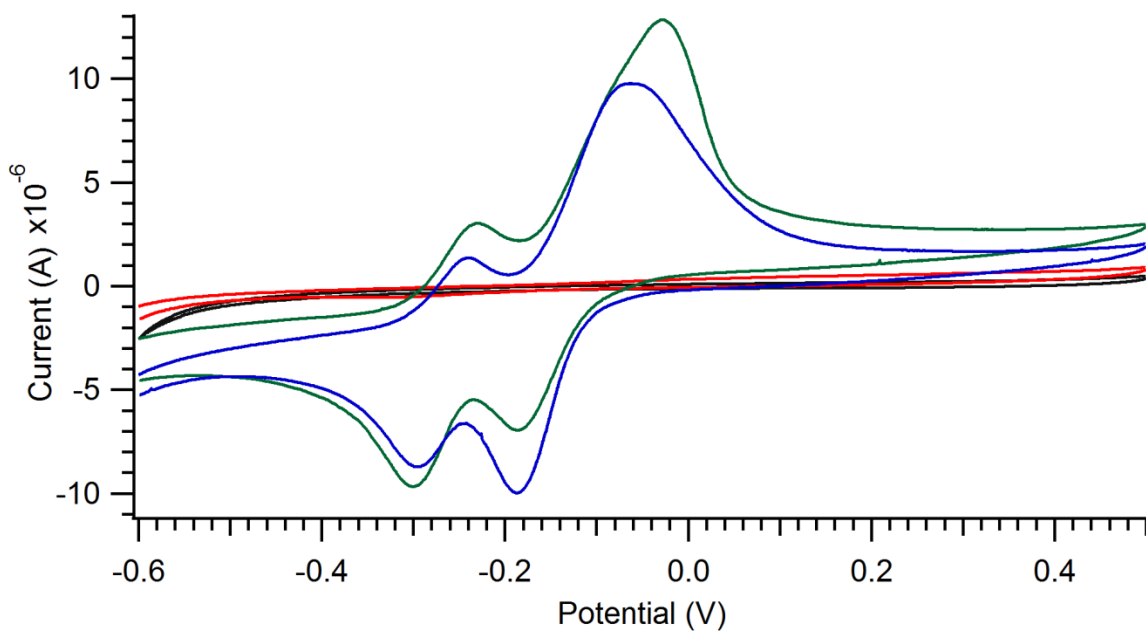


Figure 4. TLCV of methylene green and Fe(II)-TauD with methylene green. A buffer control was poised at low potential for 2 s and scanned at 10 mV/s while monitoring the current (black trace). The samples were poised at the lowest potential for 100 s and scanned at 10 mV/s. These included 225 μ M holoprotein (red trace), 499 μ M methylene green (blue trace), and 500 μ M mediator and ~200 μ M holoprotein (green trace) (8/29/12).

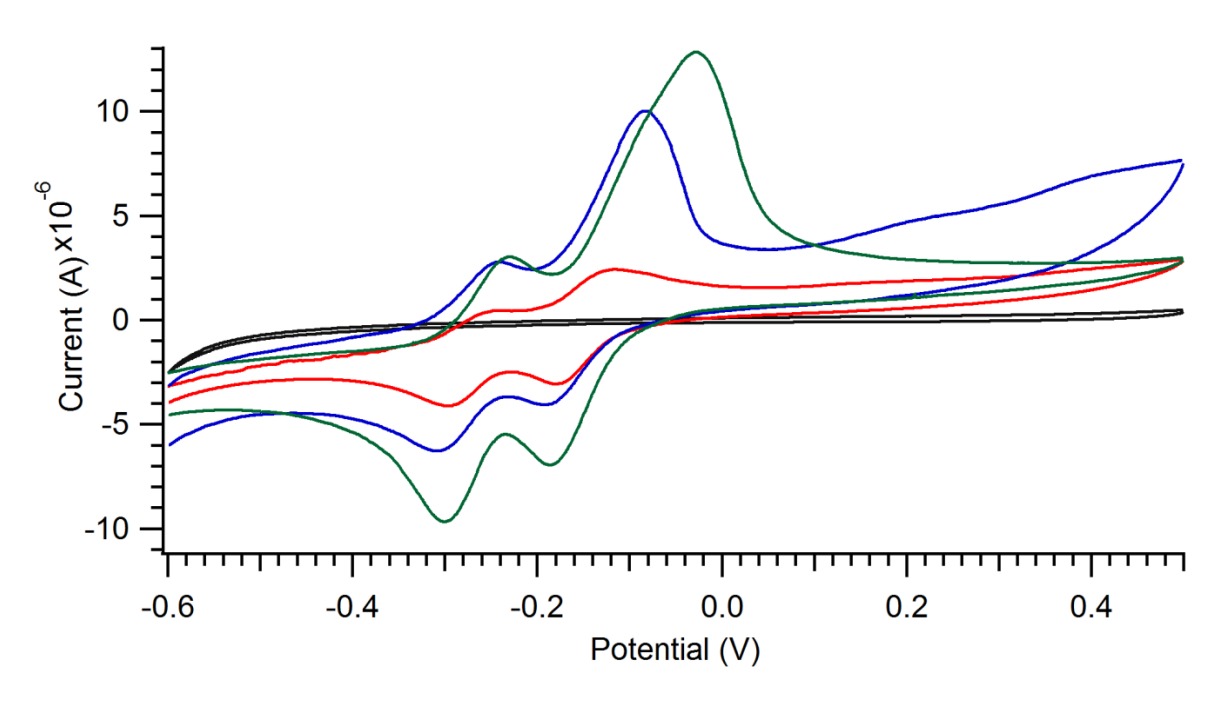


Figure 5. TLCV of Fe(II)-TauD with methylene green at various scan rates. Samples were poised at the lowest potential shown for 100 s (or 2 s for a buffer blank) and scanned. The samples included a buffer blank (black trace, 10 mV/s) or 500 μ M methylene green with ~200 μ M holoprotein scanned at 2 mV/s (red trace), 5 mV/s (blue trace), or 10 mV/s (green trace) (8/29/12).

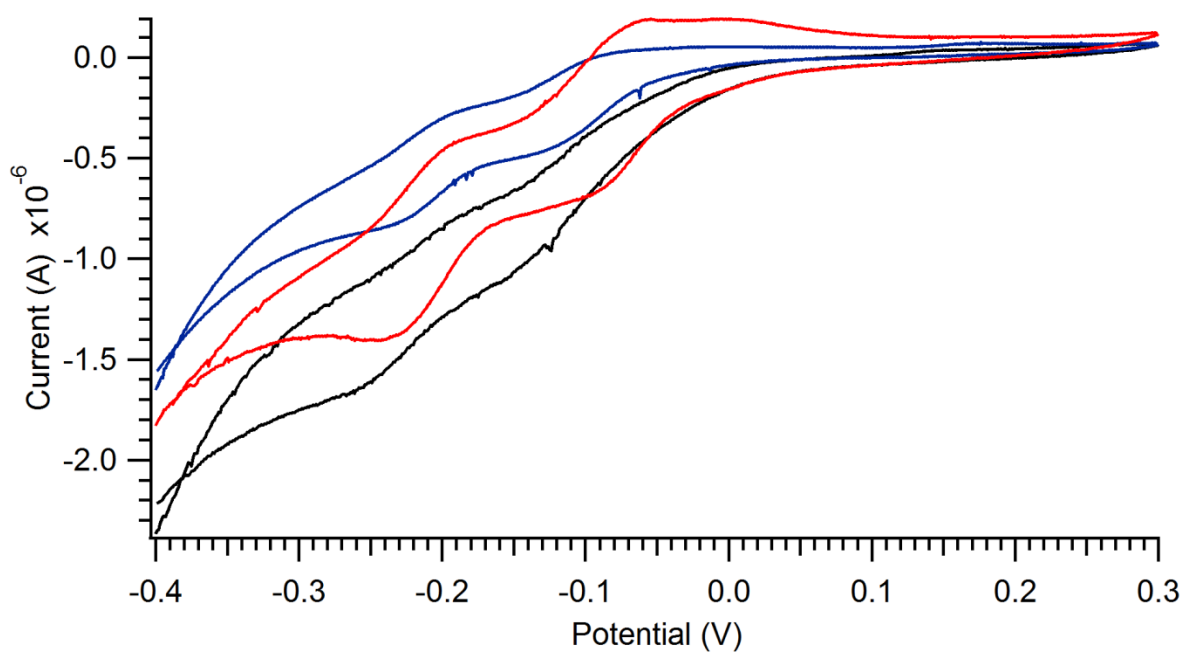


Figure 6. TLCV of Fe(II)-TauD with methylene green at a very slow sweep rate and a high protein:mediator ratio. Samples were poised at low potential for 300 s and scanned at 0.2 mV/s while monitoring the current. The samples included 52 μ M methylene green (black trace), the same concentration of mediator and 418 μ M holoprotein (red trace), and the mixture repeated on the next day (blue trace) (9/24/13).

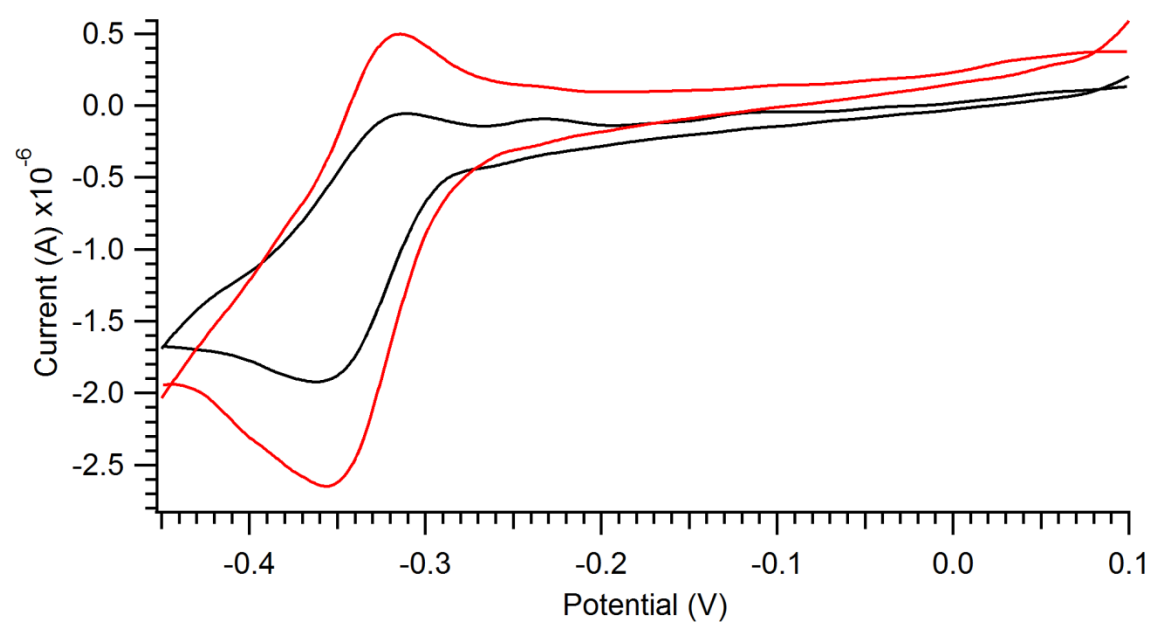


Figure 7. TLCV of methylene blue and Fe(III)-TauD with methylene blue. The samples were poised at low potential for 2 s and scanned at 2 mV/s while monitoring the current. The samples were 50 μ M methylene blue alone (black trace) and 50 μ M methylene blue plus 90 μ M Fe(III)-TauD (red trace) (12/3/12).

CHAPTER 2. MIDPOINT POTENTIAL MEASUREMENT OF TAUD: ULTRAVIOLET-VISIBLE SPECTROSCOPY TO MONITOR SPECTROPHOTOMETRIC TITRATION STUDIES

After my unsuccessful attempts to measure the midpoint potential of TauD by TLCV, I chose to use ultraviolet-visible (UV-Vis) spectroscopy to monitor titrations of a mediator into the protein mixture to estimate this value. My preliminary studies (not shown), in which I tested the ability of oxidized methylene blue and methylene green to oxidize Fe(II)-TauD and the ability of their reduced states to reduce Fe(III)-TauD, identified methylene green as the most promising candidate. Subsequent efforts involved the careful analysis of titration results using methylene green to calculate the E_m of TauD directly.

Materials and Methods

Purification of TauD

Methods were identical to those described in Chapter 1.

Preparation of Solutions

Fe(III)-TauD was prepared by degassing purified TauD apoprotein on a Schlenk line for 10-12 cycles of 1 min vacuum/1 min Ar, adding 0.9 equivalents of anaerobic Fe(NH₄)₂(SO₄)₂, and treating with 2 equivalents (an excess amount) of anaerobic ferricyanide, an oxidant that was previously shown to oxidize Fe(II)-TauD to Fe(III)-TauD (personal communication by Prof. Proshlyakov and coworkers). The ability of ferricyanide to oxidize Fe(II)-TauD was confirmed by my TLCV results (Chapter 1) which showed more current in the oxidative sweep of the experiment when the protein was present. The resulting Fe(III)-TauD was chromatographed on a PD-10 Sephadex-

G25 (GE Life Sciences) as a desalting step to remove excess ferricyanide. If needed, the desalted Fe(III)-TauD was concentrated to ~100 μM via a centrifugation step with a 10-kDa MWCO filter (Millipore). Desalted Fe(III)-TauD was degassed by 12-14 cycles of 1 min vacuum/1 min Ar.

Methylene green solid is sold (Sigma-Aldrich) in its oxidized form as the zinc chloride complex. Anaerobic methylene green solutions were prepared by adding anoxic water to degassed methylene green solid, yielding final concentrations of approximately 5 mM. Anaerobic 1 mM and 0.5 mM methylene green solutions were prepared by dilution. Solutions of oxidized methylene green (0.5 mM) were 90-95% reduced in 1.5 mL cuvettes by the addition of dithionite from a 250 mM stock solution.

All UV-Vis studies were conducted on a Hewlett Packard diode-array spectrophotometer (HP8453, Agilent Technologies, Santa Clara, CA). The cuvette holder contained a magnetic stir bar apparatus that allowed for constant stirring of the titrated solution in the cuvette. All experiments were conducted anaerobically, using degassed solutions, anaerobic cuvettes, and gas-tight syringes.

For the later experiments (those conducted after 7/2/13), I prepared the dilute solutions of protein and methylene green in an anaerobic chamber (Coy Laboratory Products, Inc., Grass Lake, MI, with a gas mix of 7% hydrogen, 10% carbon dioxide, 83% nitrogen) to ensure that anaerobic conditions were achieved and to eliminate last-minute concerns about oxygen contamination distorting my results.

Kinetics of the Reactions between TauD and Methylene Green

The kinetics of the reaction of Fe(III)-TauD and reduced methylene green were investigated according to the following methods. Aliquots of protein from a 138 µM stock

Fe(III)-TauD solution in 25 mM Tris, pH 8, were added to a dilute solution of 90% reduced methylene green (final concentration of 5 μ M) in the same buffer in a 3-mL cuvette to obtain final concentrations of 5, 10, and 20 μ M Fe(III)-TauD. The mixture was monitored spectrophotometrically over the course of 5 min, taking a spectrum every second for the first 20 s and then decreasing the time between each spectrum acquisition by 5% for the remaining period of the experiment.

Kinetics of the reaction of Fe(III)-TauD in the presence of α -KG and reduced methylene green were examined in the same manner as described above, with varying concentrations of Fe(III)-TauD (5, 10, 20, and 40 μ M) in 0.5 mM α -KG added to a dilute solution (5 μ M) of \sim 90% reduced methylene green.

Kinetics of the reaction of Fe(III)-TauD in the presence of α -KG and taurine and reduced methylene green were examined in the same manner as described above except that a concentrated solution of ~90% reduced methylene green (500 μ M) was added to a 20 μ M solution of Fe(III)-TauD in 0.5 mM α -KG and 0.5 mM taurine to obtain final concentrations of 10 μ M methylene green and 19.6 μ M Fe(III)-TauD.

Titrations of Methylene Green into TauD under Equilibrium Conditions

Thermodynamic studies of the reaction of Fe(III)-TauD with reduced methylene green were carried out in the following manner. A dilute solution (10, 15, or 20 µM) of degassed and desalted Fe(III)-TauD (see above) was prepared in a 3-mL anaerobic cuvette equipped with a stir bar. A stock solution of 0.5 mM methylene green (approximately 90-95% reduced) was titrated into the holoenzyme solutions using a gas-tight titrating syringe. After each addition of reduced methylene green, the solution was allowed to stir for 2 min to allow the reaction to reach equilibrium before acquiring a

spectrum. In the titrations of methylene green into Fe(III)-TauD in the presence of both α -KG and taurine together, the solutions were allowed to stir for 3 min to allow the reactions to reach equilibrium. Changes in the monitored absorbance intensities and the concentrations of TauD and methylene green due to changes in the volume were accounted for in the analysis of the results.

Thermodynamic studies of the reaction of Fe(II)-TauD with oxidized methylene green were conducted in the same manner, with two important differences. Fe(II)-TauD was prepared by addition of anaerobic Fe(NH₄)₂(SO₄)₂ to the anaerobic apoprotein, and the 0.5 mM stock solution of methylene green was left oxidized (no addition of dithionite). The oxidized methylene green was titrated into a dilute solution (10 or 20 μ M) solution of Fe(II)-TauD and the spectra collected 2 min after each addition (no data shown).

Results and Discussion

Determination of the Methylene Green Isosbestic Point

Methylene green proved to be the most tractable of various mediators tested for conducting UV-Vis spectroscopy studies to assess the midpoint potential of holo-TauD. This mediator has distinct spectral features in both its reduced and oxidized forms, making it easy to track its redox status during experiments with the protein. To identify the most useful features to monitor for assessing the relative levels of reduced and oxidized methylene green, I conducted an experiment to determine the mediator's isosbestic point. Dithionite was used to obtain 90-95% reduced methylene green, a spectrum was taken, and additional spectra were obtained at varied times after oxygen introduction (Figure 8). Subtraction of the oxidized spectra from the reduced absolute

spectrum produced difference spectra with maxima (260 nm) corresponding to the reduced methylene green, and minima (291 and 664 nm) corresponding to the oxidized mediator (Figure 9). These features are similar to those UV-Vis spectral features for methylene blue, a dye of similar structure [31, 34]. The intensity for the isosbestic point of the difference spectra (275 nm) represents the total amount of methylene green in the solution.

Kinetics of Electron Transfer between Methylene Green and Fe-TauD

The kinetics of electron transfer between Fe(III)-TauD and reduced methylene green were investigated for various conditions. For example, when Fe(III)-TauD was added to reduced methylene green while monitoring the appearance of the absorbance at 664 nm (associated with the oxidized mediator) the reaction reached equilibrium by 2 min (data not shown). Similar results were noted when the reaction was repeated in the presence of 0.5 mM α KG (Figure 10). In contrast, the reaction of 10 μ M reduced methylene green and ~ 20 μ M Fe(III)-TauD in the presence of 0.5 mM α -KG and 0.5 mM taurine required ~ 3 min to reach equilibrium (data not shown).

Determination of the Midpoint Potential of TauD

Methylene green that had been 90-95% reduced was titrated into solutions containing Fe(III)-TauD while monitoring the spectral changes (Figure 11). The intensities of the absorbance peak at 664 nm (baseline corrected by subtracting the absorbance at 850 nm or by using a spline between 530 and 740 nm) was assumed to correspond exclusively to the concentrations of oxidized methylene green. Similarly, the differences in absorbances between 260 nm and 291 nm reflect the concentrations of reduced methylene green. These values of the oxidized and reduced mediator

concentrations are plotted in Figure 12 over the course of the titration for mediator added to buffer alone (triangles and X, respectively) and for mediator added to a solution containing Fe(III)-TauD (diamonds and squares, respectively). As expected, the addition of 90-95% reduced methylene green to anaerobic buffer results in a linear increase in the 260-291 nm difference absorption and the 664 nm absorption. In contrast, for the sample containing Fe(III)-TauD both features were offset from these controls. Thus, the first few additions of the reduced mediator resulted in substantially more absorbance associated with oxidized methylene green and less of the absorbance for the reduced species than found with the controls. These offsets are attributed to electron transfer from the mediator to the protein. After about one equivalent of mediator was added, the titration in the presence of protein showed near linear behavior for both lines.

The midpoint potential of methylene green alone was determined to be -0.231 V vs. Ag/AgCl in a TLCV experiment (0.5 mM methylene green in a 1 M KCl solution of 50% 25 mM Tris, pH 8, 50% water in a thin layer cell equipped with a spacer of 75 µm, glassy carbon electrode as the working electrode, Ag/AgCl in 1 M KCl as the reference electrode, poised at the lowest potential for 2 s, then scanning from -0.35 V to +0.35 V back to -0.35 V at a scan rate of 5 mV/s; data not shown). The midpoint potential of TauD could then be calculated by fitting the experimental data to the best fit line, the equation of which is the modified Nernst equation (Eq. 3) in Igor Pro Technical Graphing and Data Analysis (WaveMetrics, Inc., Lake Oswego, OR, USA), using a program developed by Wen Gao and Dr. Denis Proshlyakov.

The midpoint potential of Fe(III)/Fe(II)-TauD was calculated on the basis of the equilibrium concentrations of oxidized and reduced mediator and enzyme species in titration experiments analogous to that just described, focusing on data corresponding to the Figure 12 diamonds. These data were analyzed by using a modified version of the Nernst equation that accounts for the fact that, at equilibrium, the reduction potentials of all components in a redox active system are equivalent [35]. Thus,

 $E = E_{\text{m (mediator)}} - (RT/n_{\text{mediator}}F)\ln([\text{mediator}_{\text{red}}]/[\text{mediator}_{\text{ox}}] =$

$$E_{\text{m (TauD)}} - (RT/n_{\text{TauD}}F)\ln([\text{TauD}_{\text{red}}]/[\text{TauD}_{\text{ox}}]$$
 (Eq. 2)

where $E_{\rm m}$ is the midpoint potential, $n_{\rm mediator}$ is the number of electrons lost by methylene green as it is oxidized by TauD (reduced methylene green can undergo either a one-electron or a two-electron process, so $n_{\rm mediator}$ is 1 or 2, depending on whether the methylene green product is semi-reduced or completely oxidized), and $n_{\rm TauD}$ is 1 (the Fe site in the holoprotein undergoes a one-electron transfer).

In the analysis program developed in collaboration with Wen Gao, the reaction between reduced methylene green and Fe(III)-TauD was assumed to be a one-electron transfer (i.e., n_{TauD} and $n_{mediator}$ both equal 1), producing Fe(II)-TauD and methylene green in its "semiquinone" state. Two such reactions were assumed to lead to semiquinone disproportionation (a well-described process for methylene blue [36]), generating one fully oxidized molecule and one fully reduced molecule of methylene green. Thus, for every 2 Fe(III)-TauDs reduced, one net methylene green is oxidized. In this model, Equation 2 as written above becomes

 $E_{\rm m~(TauD)} = E_{\rm m~(mediator)} - (RT/n_{\rm mediator}F) \ln([{\rm mediator}_{\rm red}]/[{\rm mediator}_{\rm ox}] + (RT/n_{\rm TauD}F) \ln([{\rm TauD}_{\rm red}]/[{\rm TauD}_{\rm ox}]$ (Eq. 3)

where n_{mediator} and n_{TauD} are equal to 1, and [mediator_{ox}] is equal to 2x [TauD_{red}]. All the results from the redox titrations of methylene green into Fe(III)-TauD with and without α -KG and taurine were fit according to this equation that describes the above model.

The results derived from four separate titrations of ~90% reduced methylene green into holoprotein alone illustrate the reproducibility of the measurements and are depicted in Figure 13. The fits of the data (red traces) were quite good. The calculated midpoint potentials over all the experiments (including several that are not depicted) yielded $E_{\rm m} = -207 \pm 27$ mV (vs. Ag/AgCl electrode). Results over various experimental preparations and concentrations of protein are shown in Table 1. The reported average represents the first measurement of the midpoint potential for any of the enzymes in the non-heme Fe(II)/ α -KG-dependent dioxygenase superfamily.

Determination of the Midpoint Potential of TauD in the Presence of Substrates

The same types of experiments were carried out to assess the midpoint potentials of TauD in the presence of α -KG and α -KG plus taurine. Experiments with α -KG (Figure 14) suggested that the midpoint potential of Fe(III)/Fe(II)-TauD does not shift significantly in the presence of the oxoacid ($E_m = -183 \pm 39$ mV). The standard deviation associated with these data is larger than for the previous sample for unknown reasons. The inclusion of both α -KG and taurine (Figure 15) generated a value that is also within the experimental deviation of the value obtained from the titration of

holoprotein alone ($E_{\rm m}$ = -210 ± 32 mV). The results of additional experiments are tabulated in Table 1, which also highlights potential issues of excess dithionite in some samples or likely oxygen contamination in other samples. Selective analysis of only the best quality data failed to improve the precision significantly (adjusted $E_{\rm m}$ of holoprotein alone = -207 ± 27 mV, of holoprotein plus α -KG = -204 ± 46 mV, and of holoprotein with α -KG plus taurine = -210 ± 32 mV).

The large standard deviations in $E_{\rm m}$ demonstrate the limits of this method used to estimate the midpoint potential of TauD. In spite of these rather large standard deviations, the lack of an appreciable shift of the midpoint potential of holoprotein when prepared in the presence of co-substrate and substrate runs counter to my original hypotheses. I expected the electron-donating effect of bound α -KG to stabilize the Fe(III) oxidation state of TauD, making the enzyme a stronger oxidant, and therefore, have a lower midpoint potential. I also expected a shift in the midpoint potential when the Fe center changed from a 6-coordinate to a 5-coordinate metal after binding of taurine and displacement of the last water coordinating to the Fe in the active site. Neither of these hypotheses were supported by the data. One interpretation of these results is that binding of the substrates does not alter the midpoint potential of the enzyme. Alternatively, one could argue that since these experiments were conducted under equilibrium conditions, I am in fact only measuring the midpoint potential of holoprotein in all three cases.

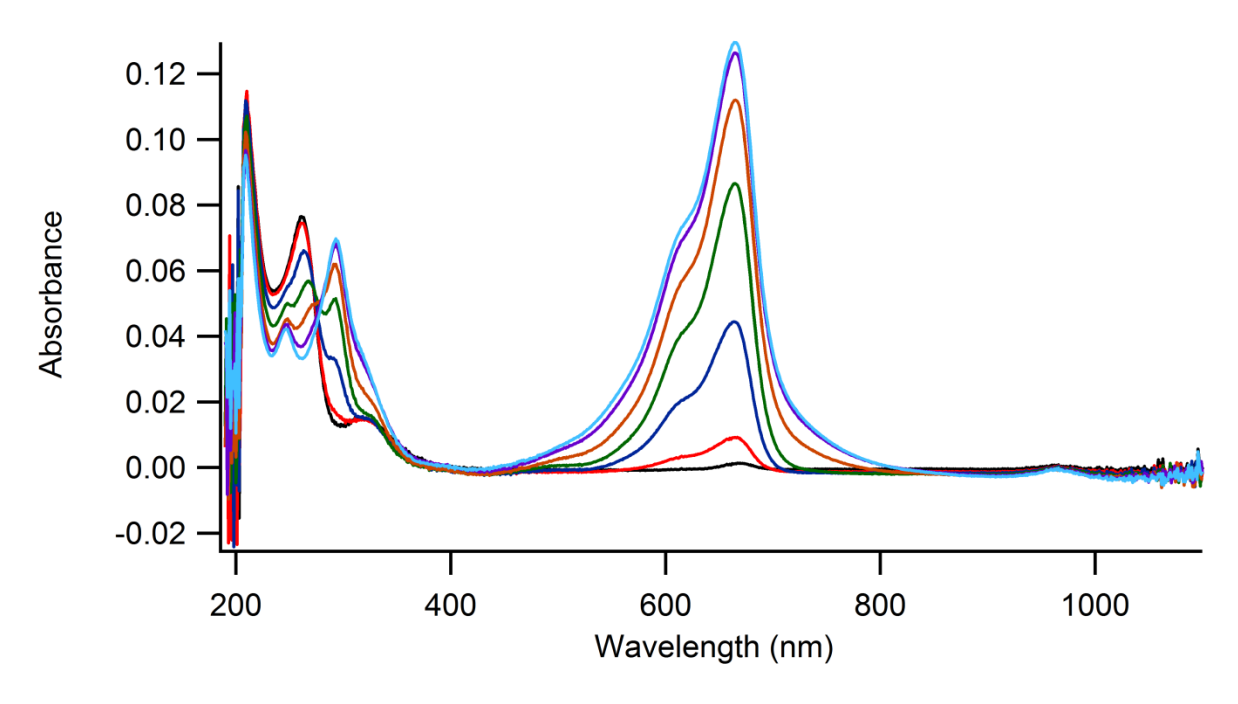


Figure 8. Absolute spectrum of reduced and air-oxidized methylene green. Methylene green (~4 μ M) was ~90% reduced with an aliquot of sodium dithionite from a 250 mM stock solution (black trace). Ensuing traces represent spectra obtained after oxygen was injected into the anaerobic cuvette, and waiting various times for oxygen to react with methylene green. The solution was constantly stirred during acquisition of the spectra.

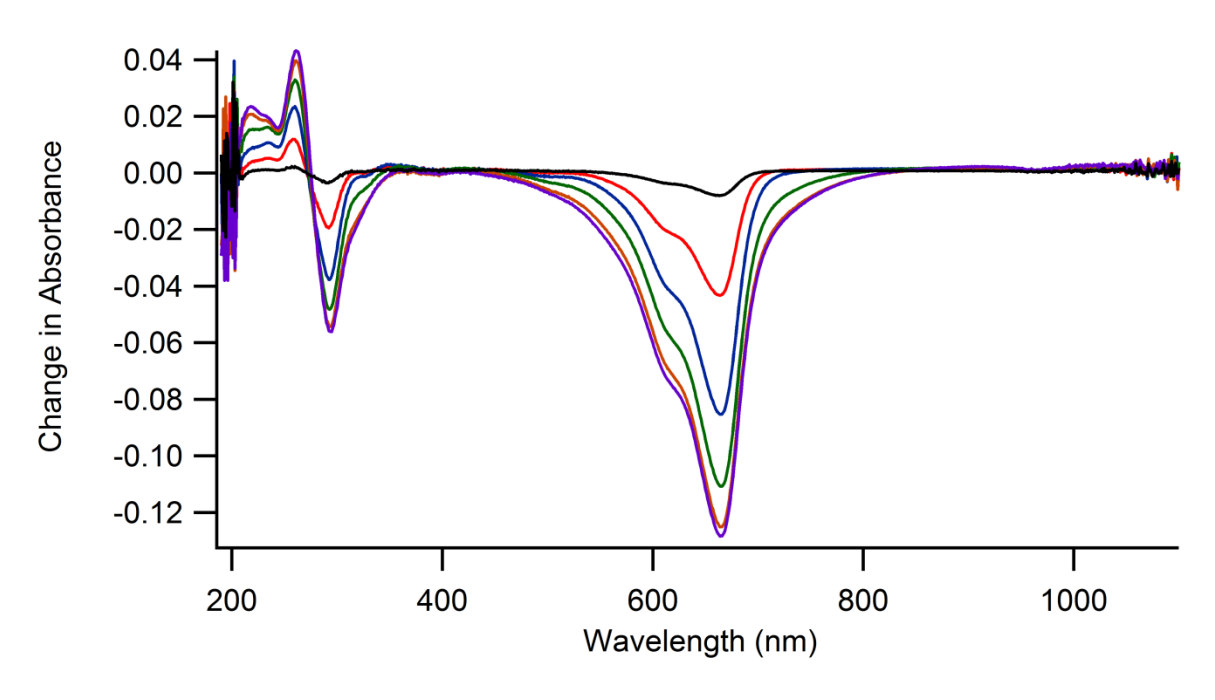


Figure 9. Difference spectra of air-oxidized and reduced methylene green. The spectra obtained during sample oxidation in Figure 8 were subtracted from the spectrum of the reduced sample.

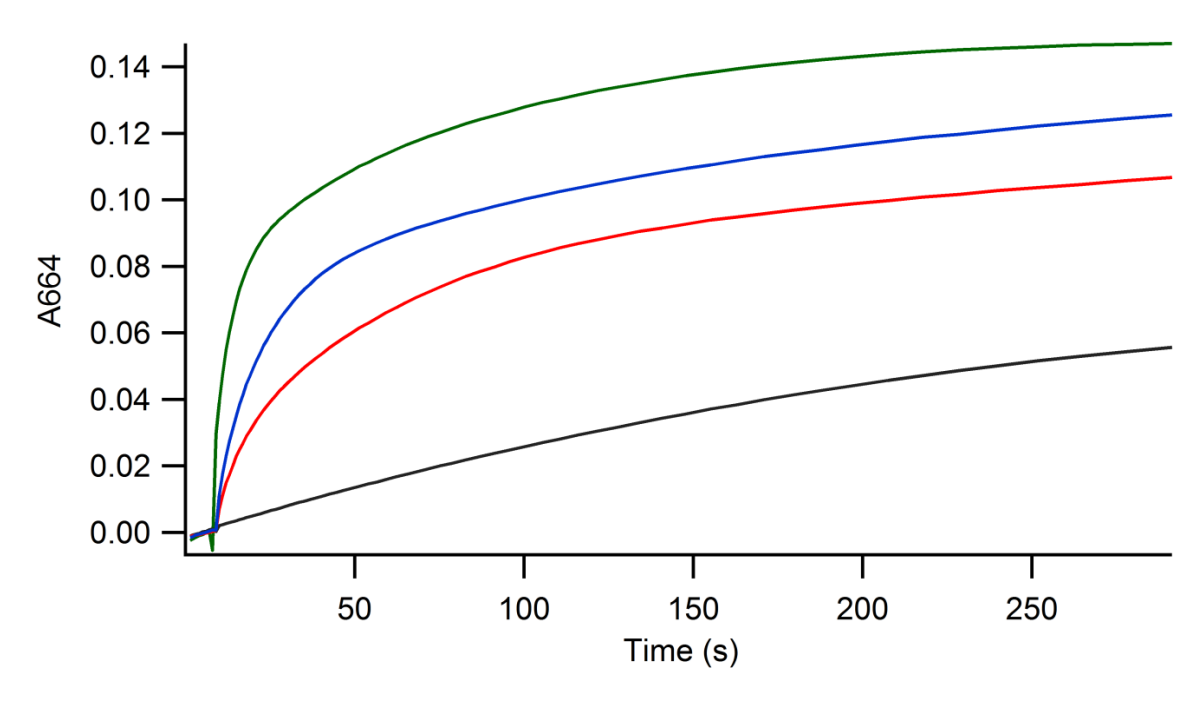


Figure 10. Kinetics of the reaction of reduced methylene green with Fe(III)-TauD plus 0.5 mM α-KG. Reaction profiles monitor the appearance of oxidized methylene green (monitored at 664 nm) after Fe(III)-TauD in 25 mM Tris/0.5 mM α-KG was added to ~90% reduced ~ 5 μM methylene green in the same buffer. An aliquot of this buffer was added to ~ 5 μM reduced methylene green as a control (black trace). An aliquot of a 90 μM Fe(III)-TauD in the same buffer was added to ~ 5 μM reduced methylene green to give final concentrations of 5 μM (red trace), 10 μM (blue trace), and 20 μM (green trace) Fe(III)-TauD in 5 μM methylene green. The reaction reached equilibrium after ~ 2 min of reaction. Absorbances are corrected for dilution (5/23/13).

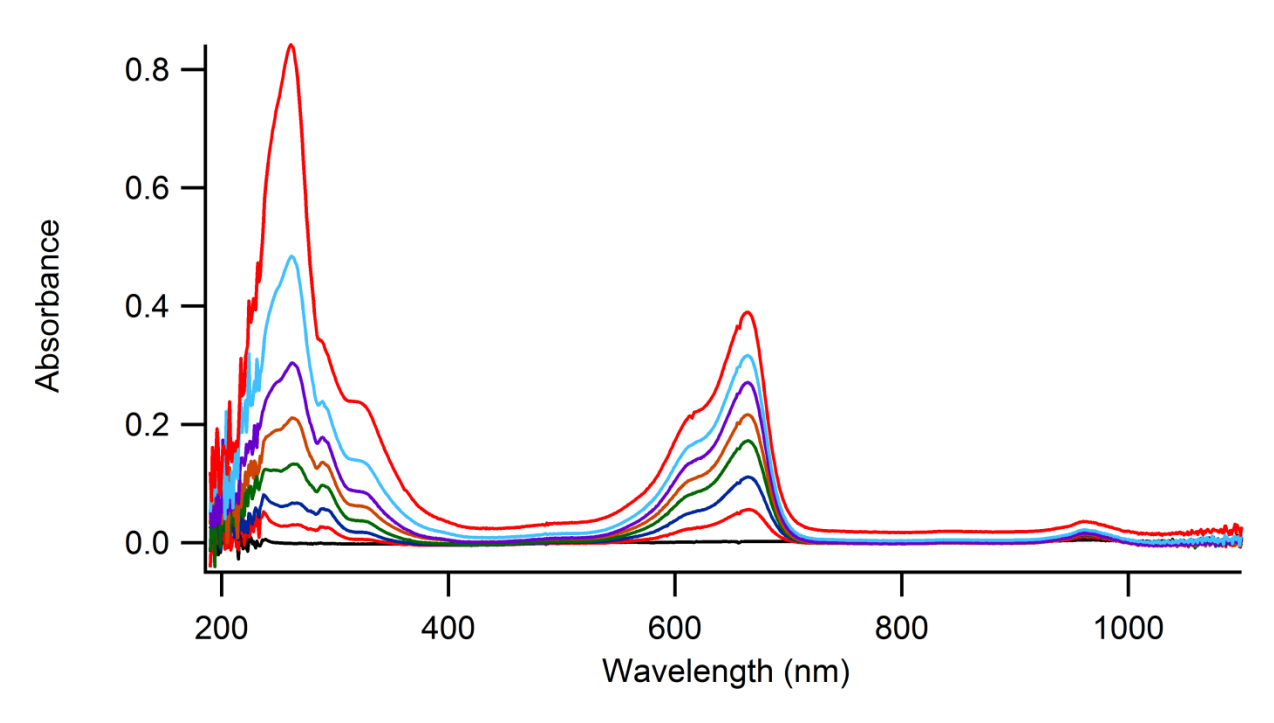


Figure 11. Absolute spectrum of the titration of methylene green into Fe(III)-TauD. The protein sample (20 μ M) in 25 mM Tris, pH 8, was amended with increasing concentrations of methylene green from a 0.5 mM stock solution with stirring and at room temperature. Absolute spectrum of blanked protein (black trace) and increasing amounts of ~90% reduced MG titrated into the protein (traces in color). Absorbances were not corrected for dilution. For this titration, the amount of oxidized methylene green was calculated from the difference in corrected absorbances at 664 nm and 850 nm (4/23/13).

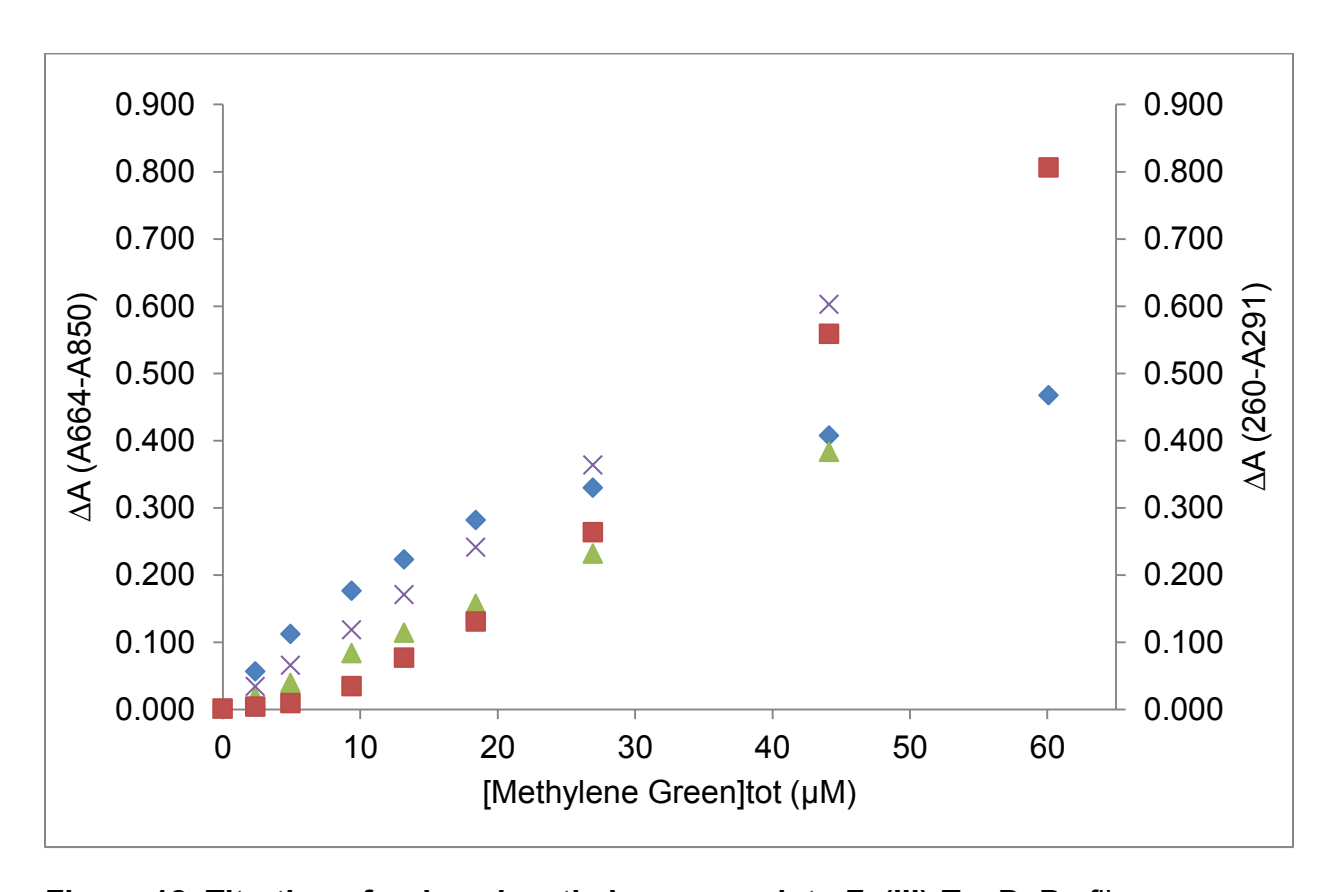
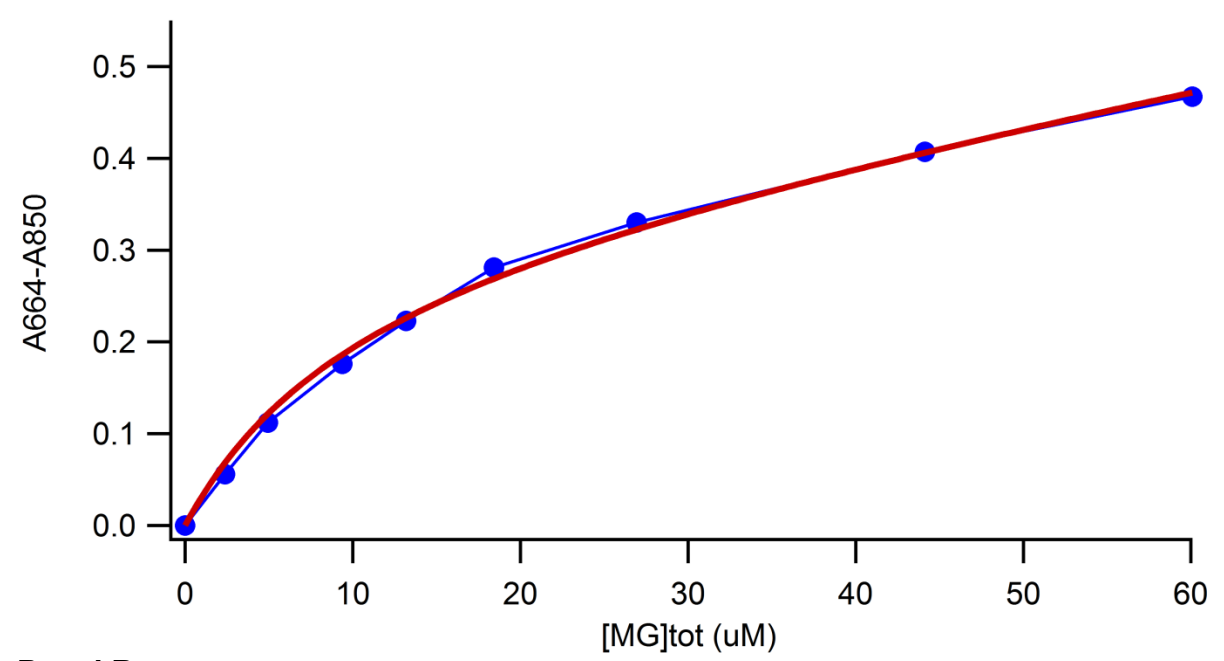
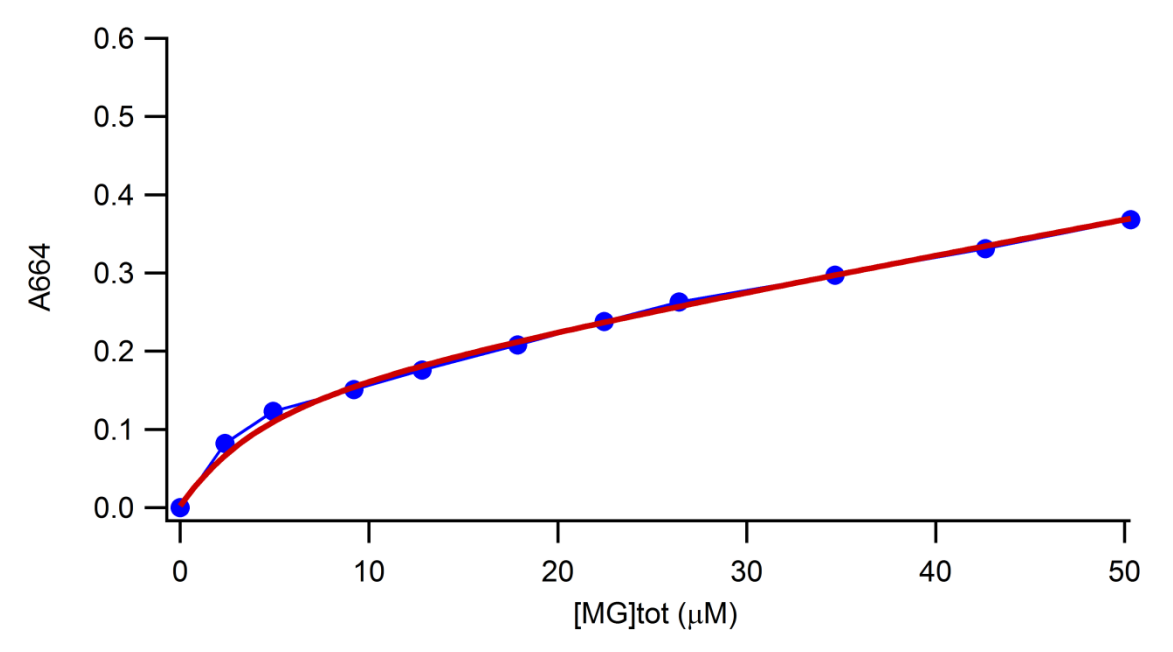


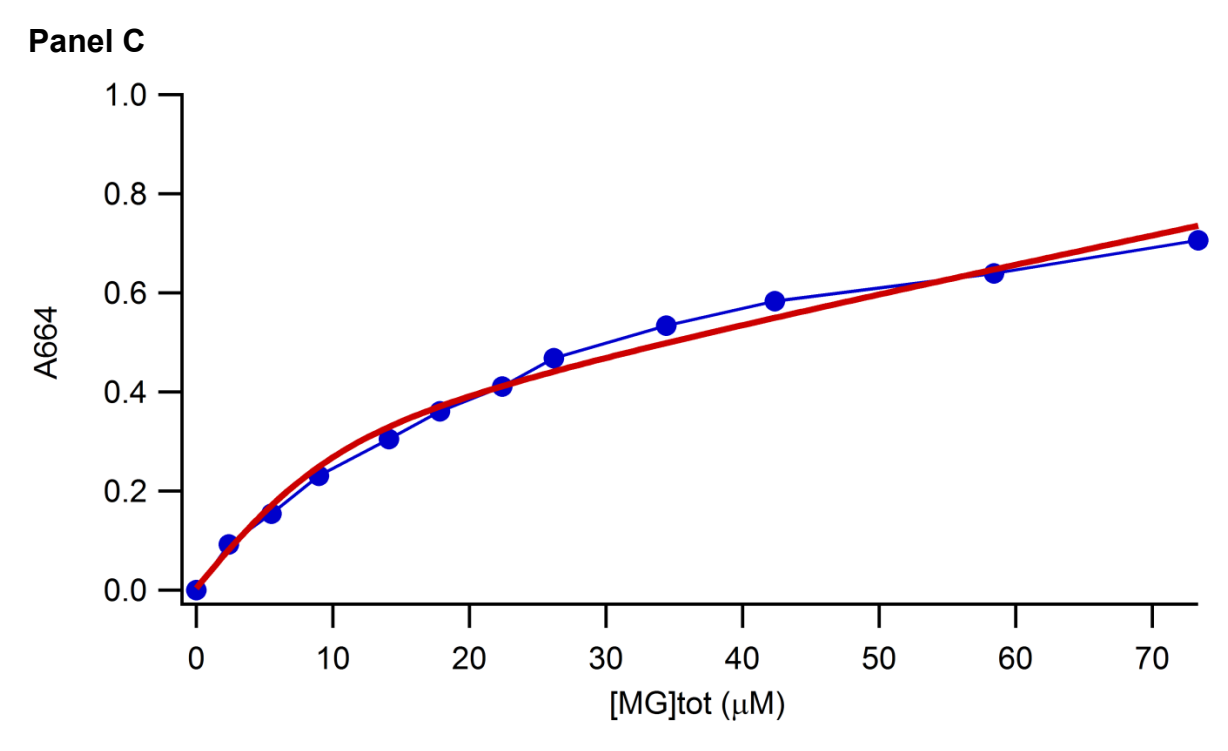
Figure 12. Titration of reduced methylene green into Fe(III)-TauD. Profiles are shown for wavelengths corresponding to oxidized methylene green (A_{664 nm} - A_{850 nm}) and reduced mediator (A_{260 nm} - A_{291 nm}) when reduced methylene green was titrated into buffer (green triangles and blue X, respectively) or into a solution containing 20 μ M Fe(III)-TauD (blue diamonds and red boxes, respectively). The absorbances were corrected for dilution.

Panel A



Panel B





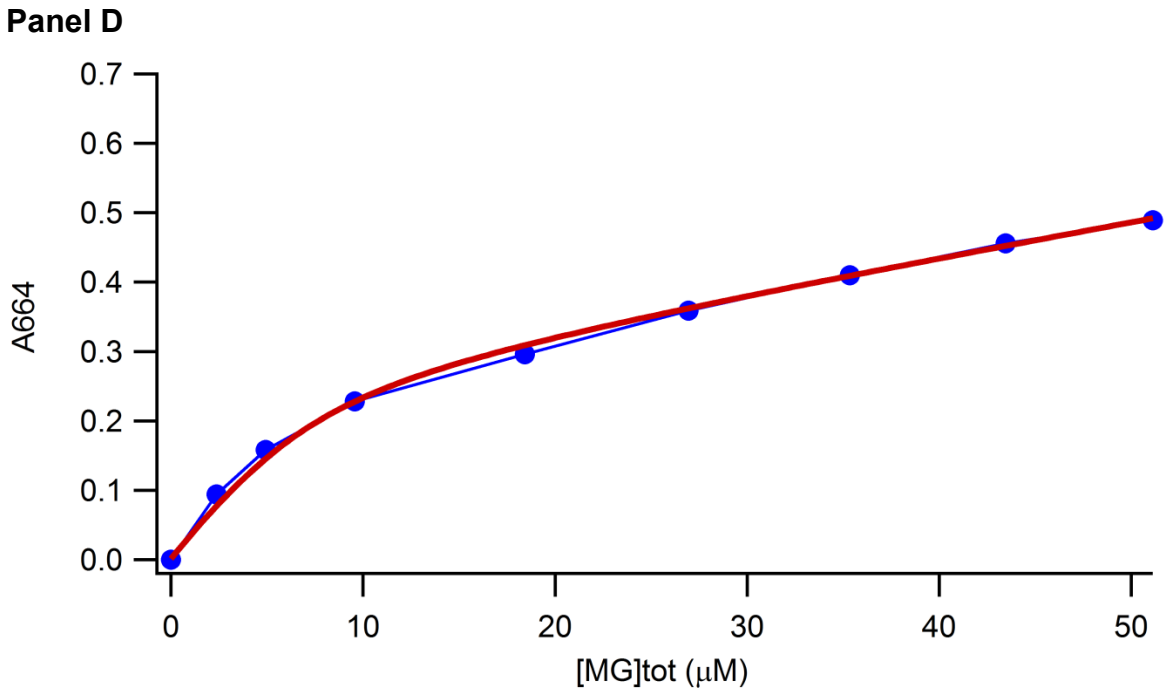
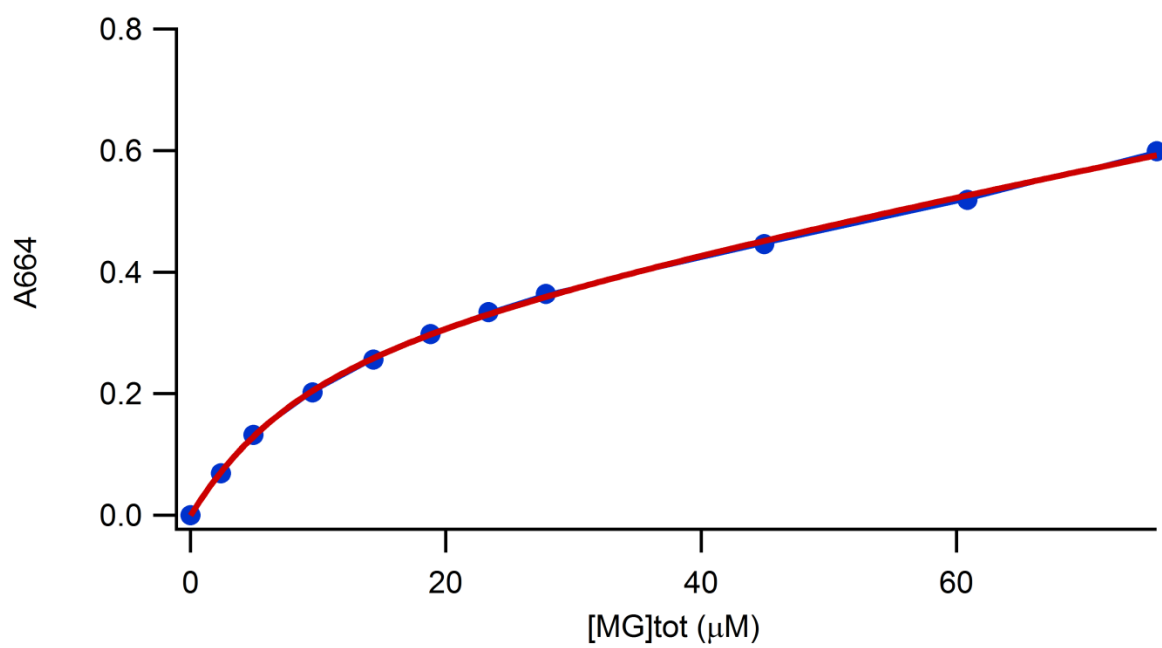
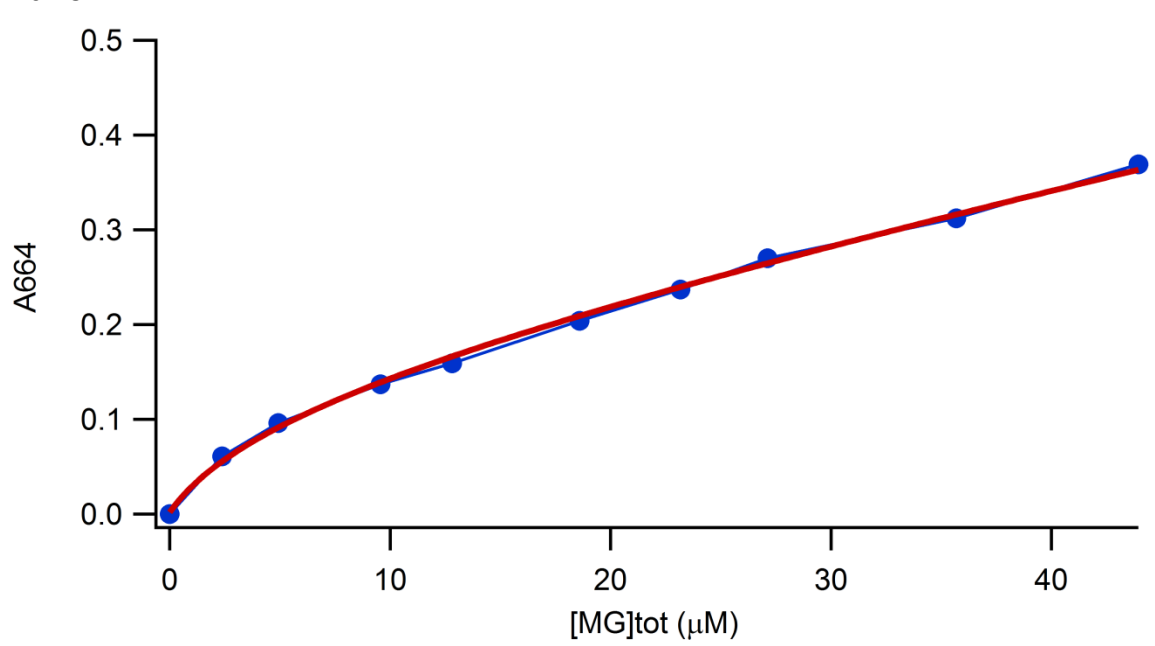


Figure 13. Titrations of ~90% reduced methylene green into solutions of Fe(III)-TauD while monitoring the concentrations of oxidized methylene green. Four replicates (blue traces with markers) are shown along with their fits (red traces). The estimated E_m values for the holoprotein (vs. Ag/AgCl electrode) in these experiments were: -227 ± 3 mV (Panel A, 20 μ M protein, 4/23/13), -215 ± 5 mV (Panel B, 10 μ M protein, 7/3/13), -187 ± 10 mV (Panel C, 20 μ M protein, 7/4/13) (Panel C), and -187 ± 7 mV Panel D, 15 μ M protein, 7/10/13).





Panel B



Panel C

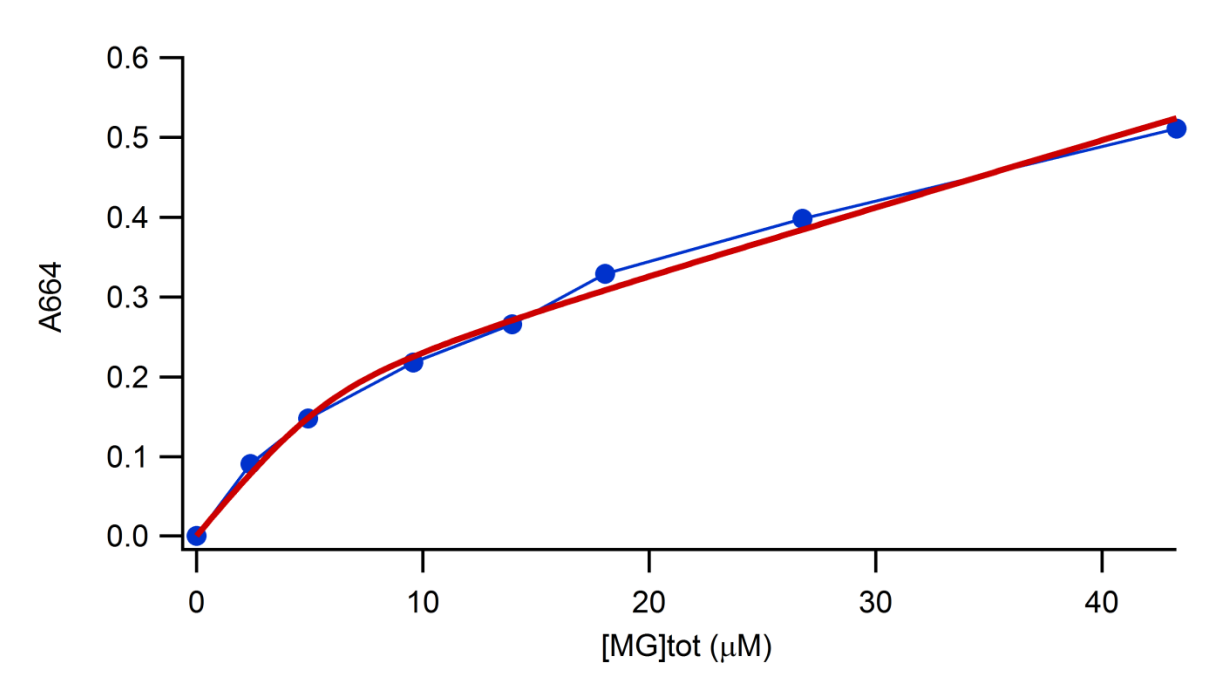


Figure 14. Titrations of $\sim 90\%$ reduced methylene green into solutions of Fe(III)-TauD plus α -KG while monitoring the concentrations of oxidized methylene

green. Three replicates are shown along with their fits. The estimated E_m values for the holoprotein (vs. Ag/AgCl electrode) in these experiments containing 0.5 mM α -KG were: -218 ± 2 mV (Panel A, 20 μ M protein, 7/8/13) and -255 ± 6 mV (Panel B, 15 μ M protein, 7/11/13), and -165 ± 27 mV (Panel C, 10 μ M protein, 7/12/13).

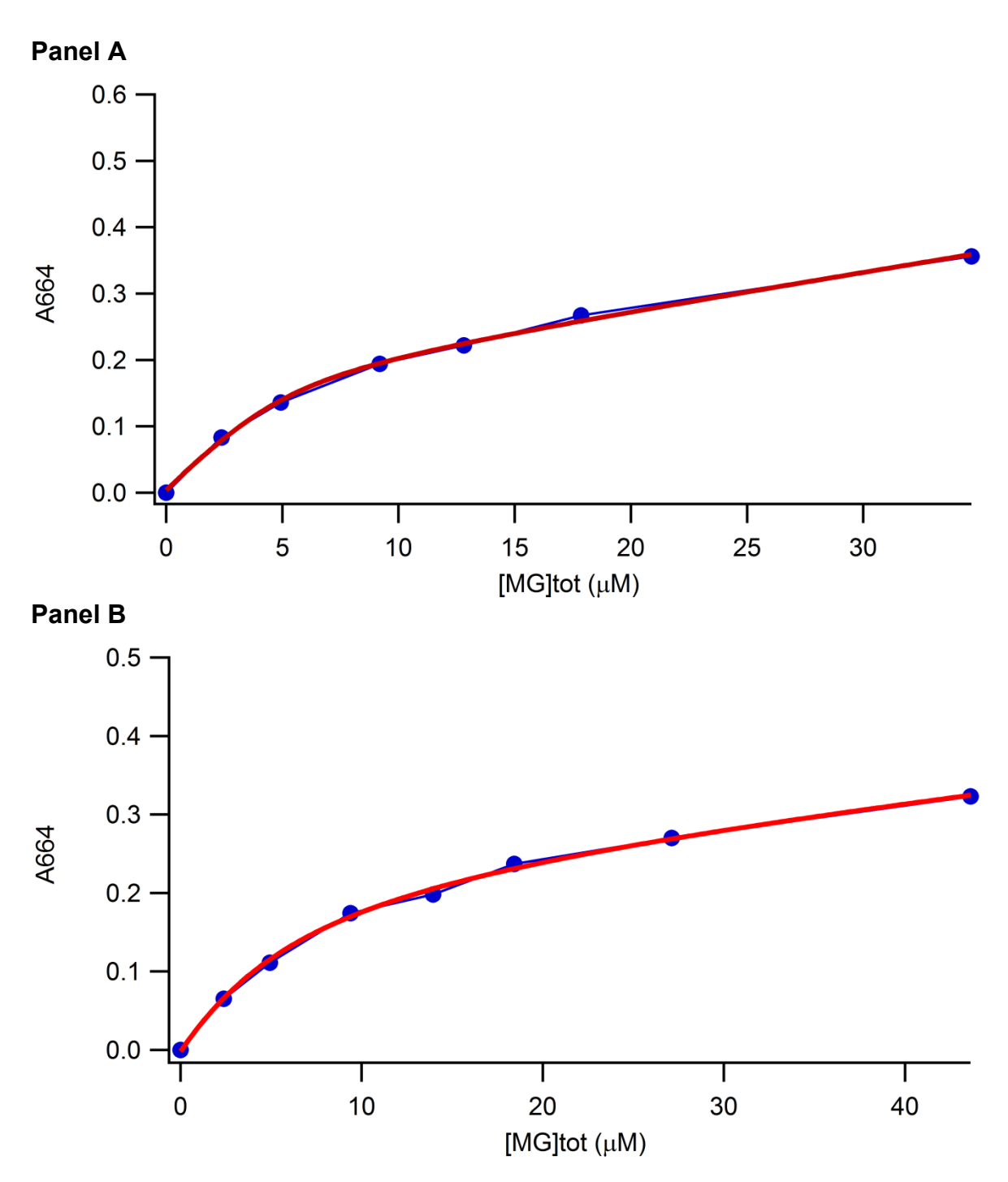


Figure 15. Titrations of ~90% reduced methylene green into solutions of Fe(III)-TauD, α -KG, and taurine while monitoring the concentrations of oxidized methylene green. Two replicates are shown along with their fits. The estimated E_m values for the holoprotein (vs. Ag/AgCl electrode) in these experiments containing 0.5 mM α -KG and 0.5 mM taurine were: -179 \pm 9 mV (Panel A,10 μ M protein, 7/5/13) and -218 \pm 4 mV (Panel B, 15 μ M protein, 7/12/13).

Table 1. Measured midpoint potentials of Fe(III)-/Fe(II)-TauD alone, with 0.5 mM α -KG, and with 0.5 mM α KG and 0.5 mM taurine. All reported midpoint potentials are in reference to the Ag/AgCl reference electrode.

Date	[Fe(III)-TauD] (μM)	E _m of Fe(III)-TauD alone (mV)	E _m of Fe(III)-TauD + α-KG (mV)	E _m of Fe(III)-TauD + α-KG + taurine (mV)
4/11/13 ¹	11	-201	-	-
4/16	10	-218	-	-
4/16 ²	20	-214	-	-
4/22	10	-258	-	-
4/23	20	-227	-	-
5/22	20	-	-171	-
5/30	20	-	-181	-
6/5 ³	20	-169	-	-
6/13 ³	10	ND ⁴	-	-
6/13 ³	20	ND ⁴	-	-
6/24 ³	20	-177	-	-
6/24 ³	20	-171	-	-
6/25 ³	20		-147	
6/25 ³	20	-	-168	-
7/2 ³	20	ND ⁴	-	-

_

¹ This experiment contained excess dithionite in the stock methylene green solution.

² In this experiment, there were issues with the spectrophotometer, which required a replacement of the deuterium lamp.

In these experiments, I was concerned with the possibility of oxygen contamination.

⁴ The midpoint potential of TauD was not determined for these experiments because I was concerned with the possibility of oxygen contamination.

Table 1 (cont'd)

7/3 ⁵	10	-221	-	1
7/4 ⁵	20	-185	-	-
7/4 ⁵	20		-	-209
7/5 ⁵	20	-182	-	
7/5 ⁵	10	-	-	-179
7/8 ⁵	20	-	-218	-
7/10 ⁵	15	-187 (-202) ⁶		-
7/11 ⁵	15	-	-255 (-252, -259)	1
7/12 ⁵	10	-	-165 (-145)	1
7/12 ⁵	15	-	-	-218 (-199)
7/12 ⁵	20	-	-	-269 (-255)
Average ± Stdev		-202 ± 27	-183 ± 39	−210 ± 32
Average ± Stdev, excluding expts with issues		−207 ± 27	-204 ± 46	−210 ± 32

_

⁵ In these experiments, the enzyme and methylene green solutions were prepared in an anaerobic chamber.

⁶ The values in parentheses were based on the measured absorbance of an aliquot of the stock solution that had been chemically oxidized or air oxidized. All other midpoint potential values reported in this table were based on the concentration of methylene green as calculated from weighing out solid and diluting it to 5 mM, 1 mM, and 0.5 mM solutions. If there is only one number in parenthesis, that value is based on the concentration of an aliquot that had been air oxidized. If there are two numbers listed in parenthesis, the first number is the value based on the measurement of an aliquot that had been chemically oxidized, and the second values is based on the measurement of an aliquot that had been air oxidized. When reporting the average midpoint potentials, I included the value in parentheses, when applicable, instead of the value obtained based on the calculated concentration of methylene green.

CHAPTER 3. CLONING, EXPRESSION, AND PROPERTIES OF A TAUD ORTHOLOG FROM A THERMOPHILE

According to the classical mechanism of TauD catalysis described in the introduction, after the abstraction of a hydrogen atom from the substrate taurine, the Fe(IV)-oxo intermediate is reduced to an Fe(III)-OH species. The resting state of the enzyme is regenerated upon hydroxyl radical rebound from the Fe(III)-OH species to form hydroxylated taurine, which immediately decomposes into the products aminoacetaldehyde and sulfite. In an expansion of this scheme, however, Raman spectroscopy studies give evidence for two other intermediates (Figure 16). In this alternative pathway, the Fe(IV)-oxo intermediate oxidizes the substrate, but instead of hydroxyl radical rebound from the Fe(III)-OH species, a yet-to-be identified basic protein residue (perhaps Asp 101 or Thr 100) deprotonates a short-lived Fe(III)-OH species, forming an Fe(III)-O intermediate [1]. This Fe(III)-O species is suggested to form an Fe(III)-alkoxo species, which then decomposes into the products, aminoacetaldehyde and sulfite.

The mechanism described above remains to be corroborated with other types of experimental evidence, and this elaboration of the scheme is currently controversial. The evidence for these two extra intermediates has been observed by Raman spectroscopy studies, but not in stopped-flow UV-Vis spectroscopy studies [15]. One possible explanation for the discrepancy between these methods is that the stopped-flow studies were carried out at 4 °C rather than the cryogenic temperatures used in the Raman studies. A solution to this controversy would be to avoid the use of cryogenic

temperatures by using an alternative approach to slow down the reaction steps and study these intermediates at temperatures above 0 $^{\circ}$ C.

A putative TauD ortholog was identified from an NCBI BLAST search of taurine catabolism dioxygenase-like genes. Entry *Mycobacterium thermoresistibile* ATCC 19527 (g.i. 357021939), identified as *M. thermoresistibile* TauD/TfdA, was aligned to *E. coli* TauD with 29% identity. If this protein functions as a TauD in the moderate thermophile (optimal temperature of 50 °C) [37], experiments could be run at temperatures that are ~50 °C less than the physiological conditions without resorting to cryogenic conditions. My goal was to generate a recombinant form of the protein and test whether it exhibits TauD activity.

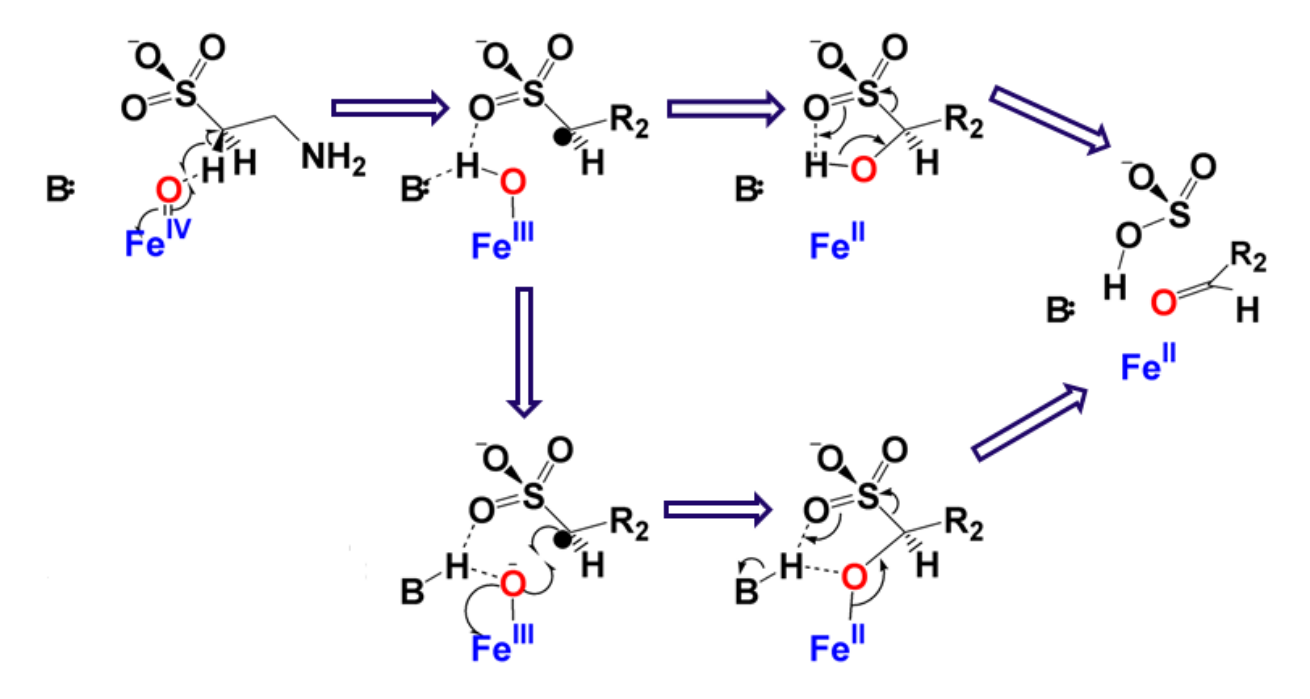


Figure 16. Alternative scheme of the decomposition of Fe(IV)-oxo intermediate and formation of products. Instead of radical rebound from an Fe(III)-OH species taking place to form the products (top arrows), Raman spectroscopic analyses provided evidence consistent with formation of an Fe(III)-O¯ intermediate and putative Fe(II)-alkoxo species (bottom arrows) that generate the products. Adapted from Grzyska *et al.* [1].

Materials and Methods

Cloning

The gene encoding the putative TauD ortholog was cloned from the *M.* thermoresistibile genome, generously provided by Dr. Christoph Grunder (University of Washington, Seattle, Washington). *M. thermoresistibile* ATCC 19527 DNA was amplified using the oligonucleotide sequences 5'-

ACGAGAAGACGAGACATATGAGCC-3' and 5'-ATCCGGGTCACTGGATCCG-3' as the forward and reverse primers, respectively. The high G/C content of the *M.*thermoresistibile ATCC 19527 gene (71% G/C) necessitated the use of "Platinum" *Pfx*DNA Polymerase (Invitrogen) to amplify the sequence from the genomic DNA. The gene was amplified on a GeneAmp PCR System 9700 thermocycler. NdeI and BamHI

restriction enzymes (New England BioLabs) were used to restrict the purified PCR product and the isolated pET-42b vector, and the fragments were successfully ligated together using T4 ligase (NEB). The resulting construct was transformed into DH5α Max Efficiency Competent Cells (Invitrogen) and the sequence was examined (Davis Sequencing, CA) using T7 and T7-terminator primers for sequencing. A frameshift was shown to have occurred during the amplification resulting in 1) loss of a stop codon in the amplified *M. thermoresistibile* gene and 2) truncation of the 3' end of the gene so it ended 3 codons prematurely.

Two rounds of site directed mutagenesis were used to correct the construct. The first round of site-directed mutagenesis substituted a codon to code for the correct amino acid and correct the frameshift mutation. The second round of mutagenesis generated a stop codon by generating two point mutations in the 3' end of the fragment corrected in the first round of mutagenesis. The construct was designated as plasmid pCW-2 and transformed into $E.\ coli\ DH5\alpha\ cells\ (Invitrogen)$ for storage as a glycerol stock at $-80\ ^{\circ}C$ and into BL21(DE3) for expression studies.

Expression of M. thermoresistibile ATCC 19527 in Recombinant E. coli

A 50-mL flask of Terrific Broth/50 μg/mL kanamycin was inoculated with pCW-2 BL21 from a Luria Broth agar/50 μg/mL kanamycin plate, and grown at 37 °C until O.D.₆₀₀ ~0.4 was obtained. The culture was divided into three sets of three 3-mL cultures. Each set of three 3-mL cultures was grown at a different temperature after induction: 16 °C, room temperature (~25 °C), and 35 °C. Within each set of three, the concentration of IPTG used to induce expression of the *M. thermoresistibile* protein was

varied to obtain a final concentration of 0.25, 0.5, and 1 mM. The cultures were grown overnight, harvested, and then lysed via sonication. The cell lysates were analyzed on 12 % SDS-PAGE gels.

Purification

Cell extracts were obtained from harvested cultures as previously described in Chapter 1. A variety of chromatographic techniques and combinations were examined, including DEAE-Sepharose, phenyl-Sepharose, gel filtration, Q-Sepharose, and hydroxyapatite chromatography. For DEAE-Sepharose followed by phenyl-Sepharose chromatography, the methods were identical to those described in Chapter 1. DEAE-Sepharose followed by hydroxyapatite chromatography was attempted as a second purification technique. The DEAE-Sepharose pool of protein was applied to a hydroxyapatite column (1.5 cm X 2.54 cm), pre-equilibrated in 5 mM sodium phosphate, pH 6.8 buffer. The application of a salt gradient (from 5 mM to 500 mM NaPO₄, pH 6.8) was used for protein elution, but the desired protein did not bind to this resin. In another purification trial, cell extract was applied to a Q-Sepharose column (2.5 X 13 cm), with the same purification protocol as described in Chapter 1 for DEAE-Sepharose chromatography. For gel filtration chromatography, cell extract was directly applied to the Superdex-200 column and chomatographed as previously described in Chapter 1. In addition, in one instance of gel filtration chromatography, 8 mM dithiothreitol (DTT) was added to the resuspension buffer used for making cell extract.

Activity Assays

Activity assays were performed as previously described in Chapter 1, except that these preliminary studies were carried out at 37 °C, 45 °C, and 55 °C. A single time point, 5 min of reaction, was chosen to assess for TauD-like activity.

Results

The *M. thermoresistibile* gene encoding a proposed taurine:α-ketoglutarate dioxygenase (abbreviated *Mth* TauD) was successfully inserted into the pET-42b vector and transformed into *E. coli* DH5α and BL21(DE3) strains; however, 5 mutations were introduced into the gene during this process. After correcting the sequence by site-directed mutagenesis, this construct, denoted as pCW-2, was successfully expressed in *E. coli* as shown by the SDS-PAGE gel (Figure 17). Furthermore, this protein was primarily expressed in the soluble fraction of recombinant *E. coli* cell extracts.

The recombinant *M. thermoresistibile* protein was subjected to a series of purification trials. DEAE-Sepharose, Q-Sepharose, phenyl-Sepharose, and gel filtration chromatography were all used in experimental trials to purify *Mth* TauD, predicted to have a molecular weight of 31 kDa. The purification protocol that met with the most success was that used for purifying *E.* coli TauD: DEAE-Sepharose followed by phenyl-Sepharose chromatography. My preliminary purification trials provided highly enriched protein (Figure 18) that was suitable for activity assays, but additional efforts are needed to optimize the purification protocol.

Attempts to detect taurine-degrading activity by *Mth* TauD were not successful.

Activity assays for TauD monitor the release of sulfite, detected by its reaction with 5,5'-dithiobis(2-nitrobenzoic acid), also known as Ellman's reagent, to release the yellow-

colored thio(2-nitrobenzoic acid). The amount of sulfite released is quantified by measuring the absorbance at 415 nm. No taurine:α-ketoglutarate dioxygenase activity was detected at the three temperatures examined. In contrast, substantial activity was noted for *E. coli* TauD which was used as a control (data not shown).

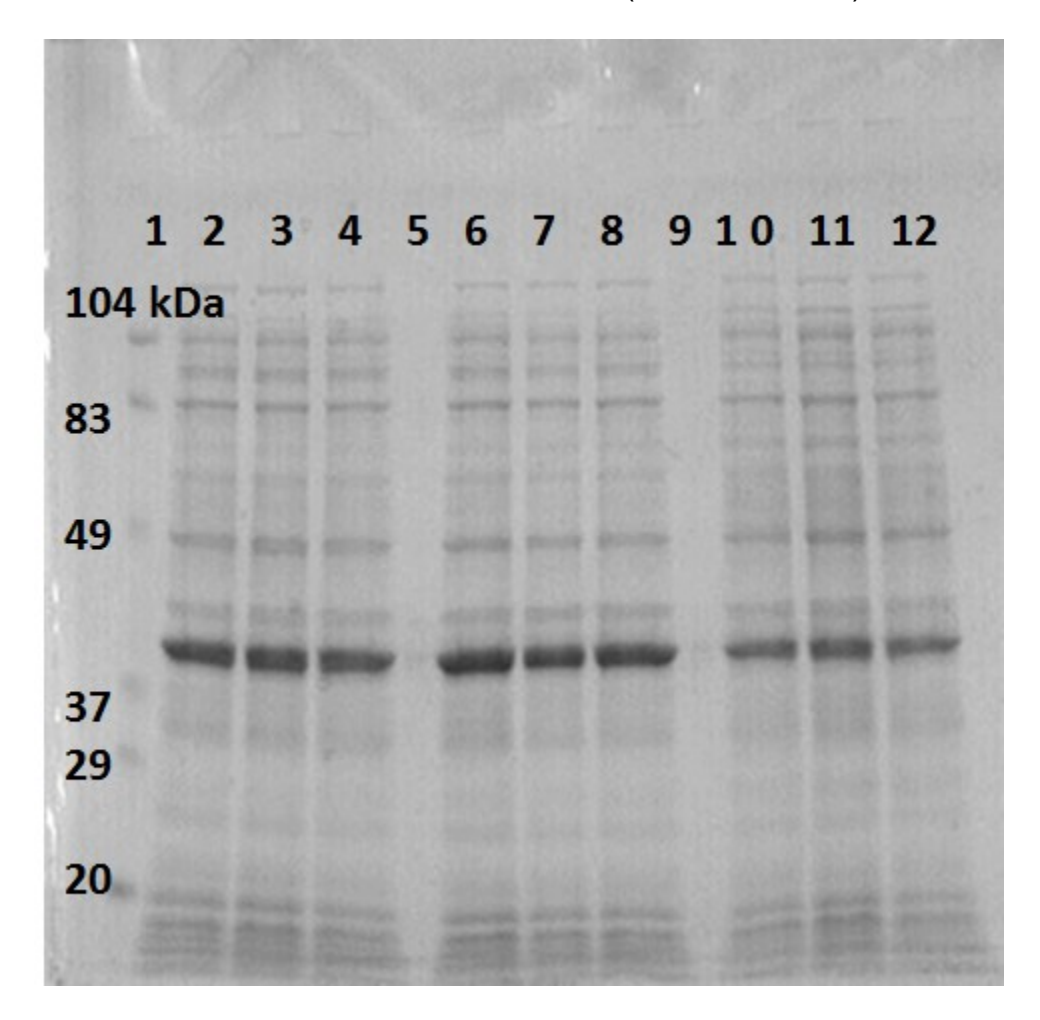


Figure 17. Initial expression of *Mth* **TauD-like protein in the supernatants of lysed** *E. coli* **BL21(DE3) cells using various induction conditions.** From left to right on the 12% SDS-PAGE gel. Lane 1: Prestained molecular mass standards (BioRad). Subsequent lanes are divided into 3 sets of conditions, with a skipped lane in between the first and second and before the third set. Lanes 2-4 contain cell extracts of cells grown at 16 °C after induction, Lanes 6-8 grown at room temperature after induction, and Lanes 10-12 grown at 35 °C after induction. Lanes, 2, 6, and 10 contain extracts from cells induced with 0.25 mM IPTG (final concentration), Lanes 3, 7, and 11 contain those induced with 0.5 mM IPTG, and Lanes 4, 8, and 12 contain those induced with 1 mM IPTG. Note: Molecular mass standards were not boiled prior to gel electrophoresis, while the samples were boiled.

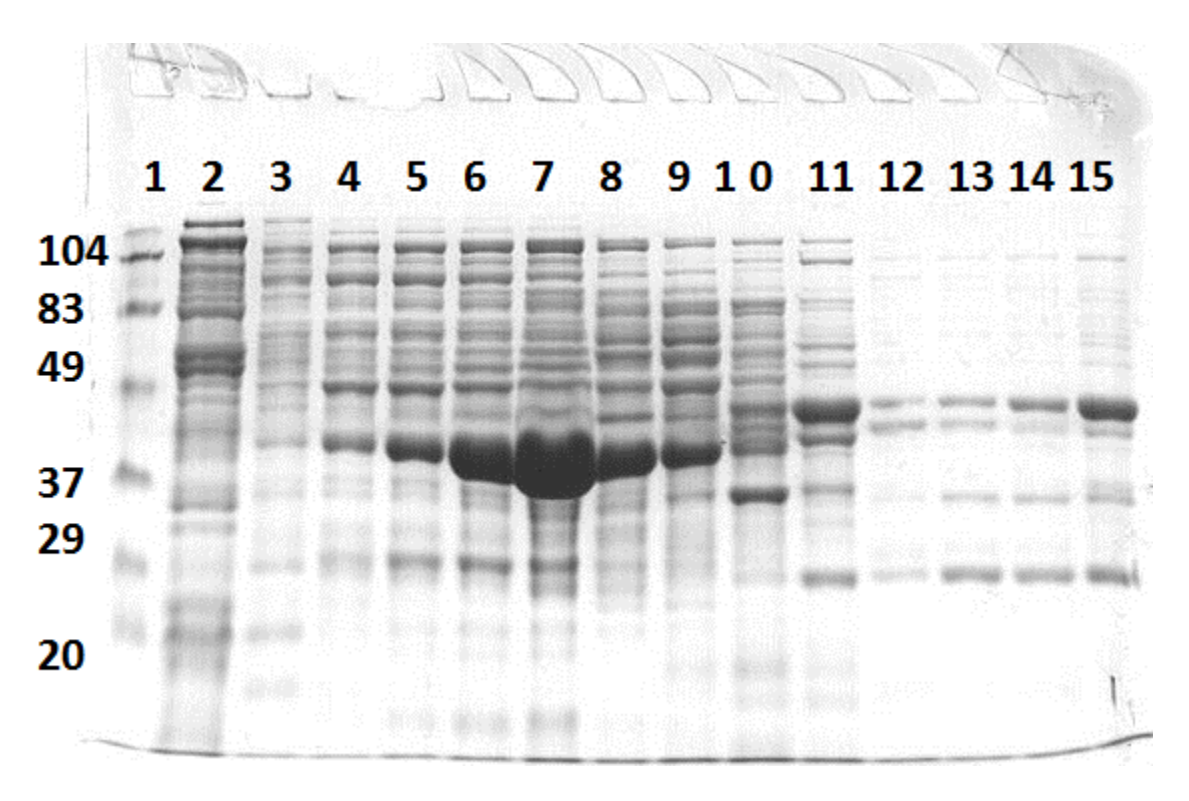


Figure 18. 12% SDS-PAGE gel of fractions eluting from a DEAE-Sepharose column. The first lane shows prestained molecular mass standards (BioRad) and subsequent lanes show fractions from the column. Lanes 6-10 contain enriched *Mth* protein. Note: Molecular mass standards (in kDa) were not boiled prior to gel electrophoresis, while the samples were boiled.

Discussion

The inability of the *M. thermoresistibile* protein to catabolize taurine can be rationalized by comparison of the residues in the substrate-binding site to that of *E. coli* TauD. The aligned sequences of *E. coli* TauD, the putative *M. thermoresistibile* dioxygenase, and two putative *Mycobacterium tuberculosis* dioxygenases, Rv0097and Rv3406 (also shown to lack TauD activity by a rotation student despite the corresponding genes being annotated as encoding taurine degradation enzymes), were analyzed relative to *E. coli* TauD (Figure 19). The critical residues at the active sites of the putative dioxygenases can be compared to the known active site residues of the *E*.

coli TauD for which the crystal structure is known with bound taurine and α-KG (Figure 20) [24].

While the TauD residues that coordinate iron in the active site (namely His 99, Asp 101, and His 255) are strictly conserved across the sequences, other critical residues at the TauD active site are not. In particular, residues critical for binding taurine in *E. coli* TauD do not match with the corresponding residues in the *M. thermoresistibile* protein. For example, Tyr 73 and Ser 158, which are adjacent to the binding site for taurine in *E. coli* TauD, are replaced by an alanine and an aspartate, respectively, in the *M. thermoresistibile* protein. Asn 95, which hydrogen bonds to taurine in *E. coli* TauD, is replaced by an alanine in the *M. thermoresistibile* protein. The only residues involved in taurine binding in *E. coli* TauD that are also conserved in *M. thermoresistibile* protein are His 70, which binds one of the sulfite oxygens, Arg 270, and Val 102. His 70 and Val 102 are not conserved across the *M. tuberculosis* putative dioxygenases.

Recent preliminary studies by others have provided evidence that the actual substrate of the recombinant *M. thermoresistibile* protein may be a sulfate, rather than a sulfonate. Compatible with this assignment a very recent publication reported that one of the *M. tuberculosis* TauD homologs is a sulfate-degrading enzyme [38]. Future studies by others could include a kinetic and spectroscopic comparison of thermophilic and mesophilic versions of this enzyme, thus meeting the original goals of this project.

```
1
    MSERLSITPLGPYIGAQISGADLTRPLSDNQFEQLYHAVLRHQVVFLR-D 49
2
    MTDLITVKKLGSRIGAQIDGVRLGGDLDPAAVNEIRAALLAHKVVFFRGQ 50
3
    -MSRLTINRLTASVGAEVTGTTADELAADAALGAAVLDALEEHGVLVFRG 49
4
    ---MTLKVKGEGLGAQVTGVDP-KNLDDITTDEIRDIVYTNKLVVLK-D 44
     QAITPQQQRALAQRFGELHIHPVYPHAEGVDEIIVLDTHNDN----PPDN 95
1
2
    HQLDDAEQLAFAGLLGTPIGHPAAIALA--DDAPIITPINSE----FGKA 94
3
    LRIDPQTQVKFCRHLGEVDHSSDGHHPVAGIYPVTLDKSKNSSAAYLRAT 99
4
     VHPSPREFIKLGRIIGOIVPYYEPMYHHEDHPEIFVSSTEEGOG-VPKTG 93
1
     DNWHTD---VTFIETPPAGAILAAKELPSTGGDTLWTSGIAAYEALSVPF 142
2
     NRWHTD---VTFAANYPAASVLRAVSLPSYGGSTLWANTAAAYAELPEPL 141
3
     FDWHIDGCTPTGDEYPQKATVLSAVQVADRGGETEFASSYGAYEALSEEE 149
4
    AFWHID---YMFMPEPFAFSMVLPLAVPGHDRGTYFIDLARVWQSLPAAK 140
1
    RQLLSGLRAEHDFRKSFPEYKYRKTEEEHQRWREAVAK-NPPLLHPVVRT 191
2
    KCLTENLWALHTNRYDYVTTKP--LTAAQRAFRQVFEKPDFRTEHPVVRV 189
3
     KRHVETLRVVHSLEASQRRVTPDPTPEQLARWRARPTH----EHPLVWT 194
4
    RDPARGTVSTHDPRR-HIKIRPSDVYRPIGEVWDEINRTTPPIKWPTVIR 189
1
    HPVSGKQALFVNEGFTTRIVDVSEKESE-ALLSFLFAHITKPEFQVR--- 237
2
   HPETGERTLLAGD-FVRSFVGLDSHESR-VLFEVLQRRITMPENTIR--- 234
3
   HRNGRKSLVLGAS--ADYVVGMDLDEGR-ALLADLLDRATTEDRVYR--- 238
    HPKTGQEILYICATGTTKIEDKDGNPVDPEVLQELMAATGQLDPEYQSPF 239
4
1
    ---WRWQPNDIAIWDNRVTQHYANADYLPQRRIMHRATILGDKPFYRAG- 283
2
    ---WNWAPGDVAIWDNRATQHRAIDDYDDQHRLMHRVTLMGDVPVDVYGQ 281
3
    ---HRWSVGDTVIWDNRGVLHRAAPYPEDSPREMLRTTVLGDEPIQ---- 281
4
    IHTOHYOVGDIILWDNRVLMHRAKHGSAAGTLTTYRLTMLDGLKTPGYAA 289
1
2
   ASRVISGAPMEIAG 295
3
    -----
4
```

Figure 19. Sequence alignment of *E. coli* **TauD with three** *Mycobacterium* **putative dioxygenases.** *M. thermoresistibile* ATCC 19527 (sequence 2), and *M. tuberculosis* Rv0097 (sequence 3) and Rv3406 (sequence 4) are aligned to *E. coli* TauD (sequence 1). Conserved ligands of Fe are underlined and bolded. Residues in *E. coli* TauD crucial for binding taurine are marked with an asterisk.

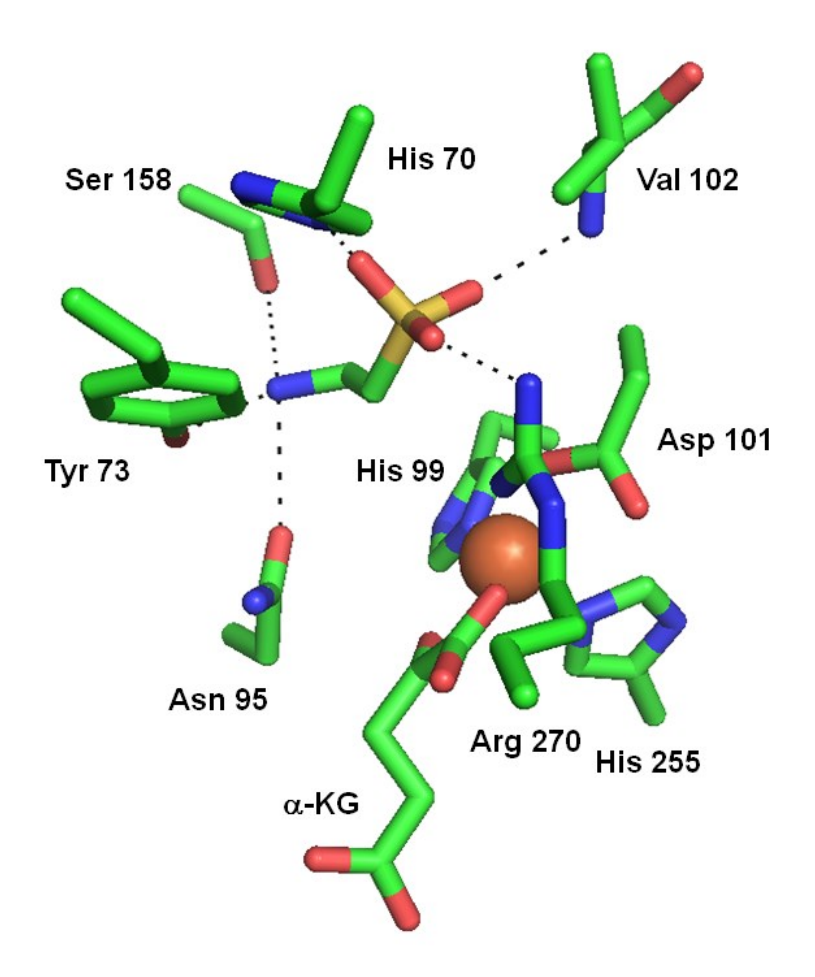


Figure 20. Taurine bound in the crystal structure of TauD with α -KG. Bound taurine (center) with hydrogen bonds (black dashes) to relevant residues. Residues of interest are shown as sticks. Fe in the active site is represented as a brown sphere. Oxygen atoms are shown in red, nitrogen atoms in blue, and carbon atoms in green. Generated from Pymol using PDB ID 1GY9.

REFERENCES

REFERENCES

- [1] P.K. Grzyska, E.H. Appelman, R.P. Hausinger, D.A. Proshlyakov, Insight into the mechanism of an iron dioxygenase by resolution of steps following the Fe(IV)=O species, Proceedings of the National Academy of Sciences, 107 (2010) 3982-3987.
- [2] R.P. Hausinger, Fe(II)/α-ketoglutarate-dependent hydroxylases and related enzymes, Critical Reviews in Biochemistry and Molecular Biology, 39 (2004) 21-68.
- [3] I.J. Clifton, M.A. McDonough, D. Ehrismann, N.J. Kershaw, N. Granatino, C.J. Schofield, Structural studies on 2-oxoglutarate oxygenases and related double-stranded ß-helix fold protein, Journal of Inorganic Biochemistry, 100 (2006) 644-669.
- [4] C. Loenarz, C.J. Schofield, Expanding the chemical biology of 2-oxoglutarate oxygenases, Nature Chemical Biology, 4 (2008) 152-156.
- [5] C. Loenarz, C.J. Schofield, Physiological and biochemical aspects of hydroxylations and demethylations catalyzed by human 2-oxoglutarate oxygenases, Trends in Biochemical Sciences, 36 (2010) 7-18.
- [6] V.M. Purpero, G.R. Moran, The diverse and pervasive chemistries of the α-keto acid dependent enzymes, Journal of Biological Inorganic Chemistry, 12 (2007) 587-601.
- [7] J.M. Simmons, T.A. Müller, R.P. Hausinger, Fe II / α -ketoglutarate hydroxylases involved in nucleobase, nucleoside, nucleotide, and chromatin metabolism, Dalton Transactions, 38 (2008) 5132-5142.
- [8] K.I. Kivirikko, T. Pihlajaniemi, Collagen hydroxylases and the protein disulfide isomerase subunit of prolyl 4-hydroxylase, Advances in Enzymology and Related Areas of Molecular Biology, 72 (1998) 325-398.
- [9] G.A. Jansen, R. Ofman, S. Ferdinandusse, L. Ijlst, A.O. Muijsers, O.H. Skjeldal, O. Stokke, C. Jakobs, G.T. Besley, J.E. Wraith, R.J. Wanders, Refsum disease is caused by mutations in the phytanoyl-CoA hydroxylase gene, Nature Genetics, 17 (1997) 190-193.
- [10] M.D. Lloyd, K.D. Merrit, V. Lee, T.J. Sewell, B. Wha-Son, J.E. Baldwin, C.J. Schofield, S.W. Elson, K.H. Baggaley, N.H. Nicholson, Product-substrate engineering by bacteria: Studies on clavaminate synthase, a trifunctional dioxygenase, Tetrahedron, 55 (1999) 10201-10220.
- [11] L. Le Marchand, Cancer prevention effects of flavonoids--a review, Biomed. Pharmacother., 56 (2002) 296-301.

- [12] E.L. Hegg, L. Que, Jr., The 2-His-1-carboxylate facial triad, European Journal of Biochemistry, 250 (1997) 625-629.
- [13] D.A. Proshlyakov, R.P. Hausinger, Transient iron species in the catalytic mechanism of the archetypal α-ketoglutarate-dependent dioxygenase, TauD, in: D. Kumar, S.P. de Visser (Eds.) Iron-containing Enzymes: Versatile Catalysts of Hydroxylation Reactions in Nature, Royal Society of Chemistry, Cambridge, U.K., 2011, pp. 67-87.
- [14] E. Eichhorn, J.R. van der Ploeg, M.A. Kertesz, T. Leisinger, Characterization of α-ketoglutarate-dependent taurine dioxygenase from *Escherichia coli*, Journal of Biological Chemistry, 272 (1997) 23031-23036.
- [15] J.C. Price, E.W. Barr, B. Tirupati, J.M. Bollinger, Jr., C. Krebs, The first direct characterization of a high-valent iron intermediate in the reaction of an a-ketoglutarate-dependent dioxygenase: A high-spin Fe(IV) complex in taurine/α-ketoglutarate dioxygenase (TauD) from *Escherichia coli*, Biochemistry, 42 (2003) 7497-7508.
- [16] P.J. Riggs-Gelasco, J.C. Price, R.B. Guyer, J.H. Brehm, E.W. Barr, J.M. Bollinger, Jr., C. Krebs, EXAFS spectroscopic evidence for an Fe=O unit in the Fe(IV) intermediate observed during oxygen activation by taurine:α-ketoglutarate dioxygenase, Journal of the American Chemical Society, 126 (2004) 8108-8109.
- [17] D.A. Proshlyakov, T.F. Henshaw, G.R. Monterosso, M.J. Ryle, R.P. Hausinger, Direct detection of oxygen intermediates in the non-heme Fe enzyme taurine/α-ketoglutarate dioxygenase, Journal of the American Chemical Society, 126 (2004) 1022-1023.
- [18] K.L. Stone, A.S. Borovik, Lessons from nature: Unraveling biological C-H bond activation, Current Opinion in Chemical Biology, 13 (2009) 114-118.
- [19] T.L. Olsen, J.C. Williams, J.P. Allen, Influence of protein interactions on oxidation/reduction midpoint potentials of cofactors in natural and *de novo* metalloproteins, Biochimica et Biophysica Acta-Bioenergetics, (2013) 914-922.
- [20] C. Léger, S.J. Elliott, K.R. Hoke, L.J.C. Jeuken, A.K. Jones, F.A. Armstrong, Enzyme electrokinetics: using protein film voltammetry to investigate redox enzymes and their mechanisms, Biochemistry, 42 (2003) 8653-8662.
- [21] T. Noll, G. Noll, Strategies for "wiring" redox-active proteins to electrodes and applications in biosensors, biofuel cells, and nanotechnology, Chemical Society Reviews, 40 (2011) 3564-3576.
- [22] J. Hirst, Elucidating mechanisms of coupled electron transfer and catalytic reactions by protein film voltammetry, Biochimica et Biophysica Acta-Bioenergetics, 1757 (2006) 225-239.

- [23] S.V. Hexter, F. Grey, T. Happe, V. Climent, F.A. Armstrong, Electrocatalytic mechanism of reversible hydrogen cycling by enzymes and distinctions between the major classes of hydrogenases, Proceedings of the National Academy of Sciences, 109 (2012) 11516-11521.
- [24] J.M. Elkins, M.J. Ryle, I.J. Clifton, J.C. Dunning Hotopp, J.S. Lloyd, N.I. Burzlaff, J.E. Baldwin, R.P. Hausinger, P.L. Roach, X-ray crystal structure of *Escherichia coli* taurine/a-ketoglutarate dioxygenase complexed to ferrous iron and substrates, Biochemistry, 41 (2002) 5185-5192.
- [25] V.D. Parker, L.C. Seefeldt, A mediated thin-layer voltammetry method for the study of redox protein electrochemistry, Analytical Biochemistry, 247 (1997) 152-157.
- [26] Y. Dai, Y. Zheng, G.M. Swain, D.A. Proshlyakov, Equilibrium and kinetic behavior of $Fe(CN)_6^{3-/4-}$ and cytochrome c in direct electrochemistry using a film electrode thin-layer transmission cell, Analytical Chemistry, 83 (2011) 542-548.
- [27] U.K. Laemmli, Cleavage of structural proteins during the assembly of the head of bacteriophage T4, Nature, 227 (1970) 680-685.
- [28] R.N.F. Thorneley, A convenient electrochemical preparation of reduced methyl viologen and a kinetic study of the reaction with oxygen using an anaerobic stopped-flow apparatus, Biochimica et Biophysica Acta (BBA) Bioenergetics, 333 (1974) 487-496.
- [29] I. Ivanov, T. Vidaković-Koch, K. Sundmacher, Recent advances in enzymatic fuel cells: experiments and modeling, Energies, 3 (2010) 803-846.
- [30] X. Li, H. Zhou, P. Yu, L. Su, T. Ohsaka, L. Mao, A miniature glucose/O₂ biofuel cell with single-walled carbon nanotubes-modified carbon fiber microelectrodes as the substrate, Electrochemistry Communications, 10 (2008) 851-854.
- [31] O. Impert, A. Katafias, P. Kita, A. Mills, A. Pietkiewicz-Graczyk, G. Wrzeszcz, Kinetics and mechanism of a fast leuco-methylene blue oxidation by copper(II)-halide species in acidic aqueous media, Dalton Transactions, (2003) 348-353.
- [32] K. Ehrhardt, E. Davioud-Charvet, H. Ke, A.B. Vaidya, M. Lanzer, M. Deponte, The antimalarial activities of methylene blue and the 1,4-naphthoquinone 3-[4-(trifluoromethyl)benzyl]-menadione are not due to inhibition of the mitochondrial electron transport chain, Antimicrobial Agents and Chemotherapy, 57 (2013) 2114-2120.
- [33] J.P. Clark, C.S. Miles, C.G. Mowat, M.D. Walkinshaw, G.A. Reid, S.N. Daff, S.K. Chapman, The role of Thr268 and Phe393 in cytochrome P450 BM3, Journal of Inorganic Biochemistry, 100 (2006) 1075-1090.

- [34] R.P. Akkermans, S.L. Roberts, F. Marken, B.A. Coles, S.J. Wilkins, J.A. Cooper, K.E. Woodhouse, R.G. Compton, Methylene green voltammetry in aqueous solution: studies using thermal, microwave, laser, or ultrasonic activation at platinum electrodes, The Journal of Physical Chemistry B, 103 (1999) 9987-9995.
- [35] Z. Cheng, L.D. Arscott, D.P. Ballou, C.H. Williams, The relationship of the redox potentials of thioredoxin and thioredoxin reductase from *Drosophila melanogaster* to the enzymatic mechanism: Reduced thioredoxin is the reductant of glutathione in *Drosophila*, Biochemistry, 46 (2007) 7875-7885.
- [36] D.W. Hay, S.A. Martin, S. Ray, N.N. Lichtin, Disproportionation of semimethylene blue and oxidation of leucomethylene blue by methylene blue and by iron(III). Kinetics, equilibriums, and medium effects, The Journal of Physical Chemistry, 85 (1981) 1474-1479.
- [37] T.E. Edwards, R. Liao, I. Phan, P.J. Myler, C. Grundner, *Mycobacterium thermoresistibile* as a source of thermostable orthologs of *Mycobacterium tuberculosis* proteins, Protein Science, 21 (2012) 1093-1096.
- [38] K.M. Sogi, Z.J. Gartner, M.A. Breidenbach, M.J. Mason J. Appel, M.W. Schelle, C.R. Bertozzi, *Mycobacterium tuberculosis* Rv3406 is a type II alkyl sulfatase capable of sulfate scavenging, PLoS ONE, 8 (2013) e65080.